To Develop the Methodology to Undertake Stock Assessments on Razor Fish Using Combinations of Video Monitoring and Electrofishing Gear

Fishing Industry Science Alliance (FISA) Project 09/15

Scottish Marine and Freshwater Science Vol 8 No 6

C J Fox

To Develop the Methodology to Undertake Stock Assessments on Razor Fish Using Combinations of Video Monitoring and Electrofishing Gear

Fishing Industry Science Alliance (FISA) Project 09/15

Scottish Marine and Freshwater Science Vol 8 No 6

Clive J Fox

Published by Marine Scotland Science

ISSN: 2043-7722

DOI: 10.7489/1908-1

Marine Scotland is the directorate of the Scottish Government responsible for the integrated management of Scotland's seas. Marine Scotland Science (formerly Fisheries Research Services) provides expert scientific and technical advice on marine and fisheries issues. Scottish Marine and Freshwater Science is a series of reports that publishes results of research and monitoring carried out by Marine Scotland Science. It also publishes the results of marine and freshwater scientific work that has been carried out for Marine Scotland under external commission. These reports are not subject to formal external peer-review.

This report presents the results of marine and freshwater scientific work carried out for Marine Scotland under external commission.

© Crown copyright 2017

You may re-use this information (excluding logos and images) free of charge in any format or medium, under the terms of the Open Government Licence. To view this licence, visit: http://www.nationalarchives.gov.uk/doc/open-governmentlicence/
version/3/ or email: psi@nationalarchives.gsi.gov.uk.

Where we have identified any third party copyright information you will need to obtain permission from the copyright holders concerned.

FISA project: To develop the methodology to undertake stock assessments on razor fish using combinations of video monitoring and electrofishing gear

Final report

Prepared by:-

Dr Clive J Fox
Scottish Association for Marine Science
Scottish Marine Institute
Dunstaffnage, Oban. PA37 1QA

Summary

Fisheries for razor clams (*Ensis siliqua* and *Ensis arcuatus*) have gone through a series of expansions in Scotland associated with changes in markets and the introduction of new harvesting techniques. Electrofishing has been recently introduced as an efficient method of forcing clams to the surface of the seabed where they can be collected by divers. Although electrofishing is illegal under European legislation the available evidence suggests that the method could be less impacting on the benthic habitat than alternate techniques, such as mechanical and hydraulic dredges. Electrofishing is also much more efficient than forcing the clams to emerge by pouring high concentration brine into the burrows (a technique known as 'salting'). Concerns over the use of electrofishing therefore relate mainly to its efficiency and the health and safety risks of using the equipment itself (potential H&S risks are not dealt with in this report). Electrofishing therefore, has the potential to lead to over-harvesting and depletion of razor clam beds, especially considering the slow growth rates of razor clams.

A further concern is that there have been very limited surveys of the stock status of *Ensis* beds around Scotland so that the impacts of harvesting would be difficult to assess. Historical stock assessments in Ireland and Scotland have mainly used dredges or salting followed by divers counting the emergent clams within quadrats[a]. As mentioned previously dredges cause damage to the habitat, as well as to the clams themselves, whilst counting using divers is slow, expensive and samples relatively small areas. The present project was designed to evaluate whether combining an electrofishing rig with a towed video-camera array could be used to assess the razor clam resources in a bed in an efficient manner.

Eighteen tows of between 30-60 mins duration were conducted at three sites. Cameras mounted on a sled were towed 2 m behind a commercial electrofishing rig using the fishing vessel 'Lizanna'. Tows were undertaken in the summer and autumn of 2016 at sites close to the Isle of Barra in the Outer Hebrides - south of the Isle of Fuday on 9th August, to the south-east of Fuday on 10th August and 1st October and in the Sound of Eriskay on 2nd October. The videos were subsequently processed using bespoke programs to correct for camera lens distortion and to relate video frame number with the estimated distance that the cameras had moved along the tow-track.

[a] A quadrat is a normally square frame which defines a set area, for example 1 m^2. Quadrat-based sampling is widely used in ecology for assessing the abundance of sessile organisms.

The quality of the videos was generally high and clams and other benthic organisms could be easily identified, counted and measured. The cameras did become obscured on a few tows by seagrass and macroalgae. This problem was more significant at certain sites and led to shorter durations on some tows. Useable data were obtained from all 18 tows.

Razor clams were identified and measured from the videos using interactive software written for the project. Resulting size frequency data were compared with samples of live clams collected by diver on three of the tows. These comparisons showed good agreement between video-based razor clam lengths and live measurements suggesting that the technique could be used to estimate both the abundance and the lengths of clams within reasonable margins of error.

As well as stationary clams we observed a proportion of the *Ensis* on the videos moving across the seabed by foot-kicking, or righting themselves and reburying. This suggests that electrofishing does not cause damage to the clams, at least in the short-term. The electrofishing-camera rig appeared to create little habitat impact apart from the shallow tracks generated by the electrodes and some dragging of weed caught on the towed gear.

The video data were also analysed in terms of the spatial clustering of clams along the tow tracks and inferences made regarding the precision of mean density estimates with variations in tow length and replication. These considerations should aid the design of future surveys if the combined electrofishing-video technique were to be more widely deployed as a stock assessment tool.

We conclude that the combination of electrofishing with towed video is a promising tool for assessing the status of razor clam beds without causing excessive damage to the habitat or the clams. However, some predation of recovering organisms may occur as large numbers of shore crabs (*Carcinus maenas*) were seen on the videos. Two instances of shore crabs attacking stunned clams were observed but the full recovery of the clams was not monitored in this project so the rarity of observed predation in the videos may underestimate actual predation rates.

Introduction

Razor clams (colloquially known as ‘spoots’) are found in fine to coarse sands down to water depths of around 20 m (Holme 1954, Fahy et al. 2001). There are two main commercial species in Scotland, *E. siliqua* and *E. arcuatus*. The former tends to be found in fine to muddy sands whilst the latter prefers coarser grained sediments (Breen et al. 2011). *E. siliqua* reach larger sizes (up to 200 mm shell length) and are distinguished from *E. arcuatus* by their lack of curvature along the ventral margin. The maximum shell lengths of *E. arcuatus* tend to be around 150 mm, although a few larger specimens have been recorded. Another smaller species (*E. ensis*) is found around the UK but is not so commercially important (Holme 1951). The differences in shell curvature between the three species are less obvious in small specimens and taxonomic identification can be problematic at these sizes (Henderson & Richardson 1994).

Based on determining the age of animals from shell markings (Henderson & Richardson 1994), suggested that both *E. siliqua* and *arcuatus* approach asymptotic size after around 10 years (Fahy & Gaffney 2001, Fahy et al. 2001). The growth rates of male and female clams also tend to be slightly different. Similar growth results have been obtained for razor clams from the Western Isles (Marine Laboratory 1998). Some animals as young as three years old have been found to be mature in Irish samples (Fahy & Gaffney 2001, Fahy et al. 2001) but full maturation probably does not occur until around five or six years of age. Both the growth rates and maturation appear to be faster in areas of southern Europe, such as Portugal, probably as a result of warmer water temperatures (Gaspar & Monteiro 1998).

All razor clams possess a strong muscular foot which is used for burrowing but can also propel the animal across the surface of the seabed. *E. siliqua* normally occur close to the surface but will respond to threats by burrowing to around 60 cm depth (Gaspar et al. 1998). It is also thought that the animals may move deeper in the sediment during periods of poor weather (Fahy & Gaffney 2001), an idea which was also supported by the fishers we worked with on this project. McKay (1992) noted that unexploited beds were often dominated by older animals (up to 25 y old) with few smaller shells being present. McKay (1992) went on to suggest that the presence of larger shellfish might suppress recruitment of smaller shellfish by consuming settling spat. However, the wording in that report is ambiguous and might refer to species other than *Ensis.* However, Fahy & Gaffney (2001) repeated the recruitment limitation hypothesis for razor clams but also suggested that such observations could arise due to mass immigration of similarly sized animals. The mobility of razor clams has been frequently mentioned so that immigration may allow re-population of harvested areas, providing there are sufficient clams in surrounding areas.

Razor clams have long been harvested by hand from the inter-tidal zone for local consumption but the development of more sophisticated fishing methods has led to increased exploitation. Although widely distributed around the UK and Ireland, clam densities only reach levels sufficient to justify commercial harvesting in certain locations (Holme 1954, McKay 1992, Marine Laboratory 1998). Unfortunately this spatial concentration can attract fishers into a restricted area, potentially leading to rapid depletion of the resource. Signs of over-exploitation, such as declines in the abundance of larger animals, failure of re-colonisation of harvested areas, overall reductions in landings and changes in benthic community composition have been historically recorded for beds in Ireland (Fahy & Gaffney 2001, Fahy and Carroll 2007), North Wales (Henderson & Richardson 1994) and Portugal (Gaspar & Monteiro 1998). Since relatively little seems to be known about natural recruitment variability in *Ensis* (Breen et al. 2011) such changes cannot be unequivocally ascribed to fishing, although the observations are consistent with over-harvesting. There are therefore, good reasons for concern regarding the sustainability of razor-clam fisheries, especially when new, highly efficient harvesting techniques are introduced.

In the 1990s, Spain and Portugal provided the main markets for the Irish and Scottish razor-clam fisheries (Fahy & Gaffney 2001) but this declined in the early 2000s. In recent years there has been growing demand for razor clams from the Far East and this now appears to the main destination for the majority of the Scottish product. These changes in demand help to explain the historical pattern in Scottish landings which increased steadily during the 1990s (Marine Laboratory 1998), fell back in the early 2000s (Murray et al. 2014) but then increased once more, reaching a peak at 915 tonnes (£3.1 million) in 2013. Reported landings have since fallen back to 350 tonnes (worth £1.6 million) in 2015 (Marine Scotland 2016). Commercial razor fishing in Scotland has mainly used suction (Marine Laboratory 1998) or hydraulic dredges (Hauton et al. 2007) or the salting method. This latter technique is quite laborious and slow and is likely to be less efficient than dredge-based methods, although causing little habitat impact and yielding a higher-quality product (Constantino et al. 2009). Allocating reported razor clam catches to fishing method is difficult but, based on analysis of data for the late 2000s (Breen et al. 2011), the reported landings probably divide about 50:50 between hand-diving and some form of mechanical extraction. Electrofishing emerged in the early 2000s (Breen et al. 2011) as a novel technique for forcing razors to the surface allowing them to be more easily collected by divers. The technical details of the method are discussed in

Breen et al. (2011) and Murray et al. (2014). Whilst electrofishing is illegal under European fisheries legislation (EU Regulation 850/98, Article 31), there was a period when this activity became quite widespread on the Scottish west coast (Murray et al. 2014). In recent years increased enforcement has led to a decline but the inshore industry has lobbied for it to be legalised. Electrofishing is attractive compared with alternative razor-clam harvesting methods since it produces good yields of high quality (negligible shell damage or internal grit) animals (Woolmer et al. 2011, Murray et al. 2014). Previous studies have further suggested that the form of electrofishing used has low impacts on other organisms and the benthic habitat (Woolmer et al. 2011, Murray et al. 2014). The concerns about legalising this fishing technique therefore relate mainly to its high efficiency and the potential for excess harvesting which could lead to rapid depletion of the stocks (in addition there are health and safety aspects which are out-with of the scope of the present project).

Having reliable estimates of the state of the resource is a normal pre-requisite for setting appropriate fisheries management targets. Stock assessments repeated over time also allow monitoring of how the resource state is changing. Changes in stock status can be inferred to some extent from shifts in the commercial catches but additional direct monitoring of the resource is extremely desirable. This is particularly the case where accurate estimation of effort is not available since catches are affected by changes in both stock status and fishing effort. Historically, attempts have been made to estimate razor clam density *in situ* using divers to observe the characteristic sediment plumes produced by the clams during escape responses (Marine Laboratory 1998). However, most razor-clam stock assessments have used either mechanical or hydraulic dredges (McKay 1992, Gaspar et al. 1998, Marine Laboratory 1998, Hauton et al. 2007), or diver-based salting followed by counting of emergent animals (Fahy et al. 2001). All these techniques have disadvantages as stock assessment tools. For example, mechanical and hydraulic dredges cause habitat damage and can also damage escaping clams, which probably do not survive (McKay 1992, Gaspar et al. 1998, Marine Laboratory 1998). Fahy and Gaffney (2001) noted that smaller razor clams were not sampled by the commercial dredges they employed so this important component of the population could not be included in their assessment. Diver-based surveys are slow and expensive and spatial coverage is likely to be low (Fahy et al. 2001). Since electrofishing seems to be a highly efficient method of forcing razor clams of all sizes from their burrows (Murray et al. 2014), it could form the basis of a more accurate, less damaging, stock assessment technique. Studies to date suggest that the majority of razor clams recover and re-bury within 10 mins of the electric field passing (Woolmer et al. 2011, Murray et al. 2014).

Overall the available evidence suggests that electrofishing might provide a novel approach to assessing razor clam stocks without causing substantial incidental damage to either the clams, non-target organisms or their habitat. The aim of this Fishing Industry Science Alliance funded project was therefore to investigate whether electrofishing could provide a practical approach to assessing stocks of razor clams and what the likely precision and financial costs of using this technique for stock assessments. A further advantage would be if the method could be operated using commercial fishing vessels since this could increase the involvement of the inshore industry in managing the resources they exploit.

Project Objectives and Extent to which the Objectives were Completed

1. To develop and trial video recording alongside electrofishing as a method for the collection of data on *Ensis* species composition, abundance and size for the purposes of stock assessment – **Completed** – a towed video sled was constructed and deployed over four days from the fishing vessel 'Lizanna'. In total, 18 tows were completed on three separate razor-clam beds. Bespoke software was written in Matlab to enable processing of the video files. Razor clams were identified on the video and their lengths and positions along the tow-track estimated.
2. Evaluate the data to determine the relationship between sampling effort and precision of abundance estimates produced – **Completed** – a boot-strapping approach was used to simulate the likely precision around mean abundance estimates with varying levels of tow length and replication based on the video data collected.
3. Produce guidance on the likely costs of conducting stock assessments on *Ensis* using this approach in inshore waters – **Completed** – Indicative costs in terms of equipment and the staff time required to collect and analyse the video data are provided in this report. A final cost in £ per survey could not be provided because staff costs are likely to vary between potential survey providers. The exact costs of producing a stock assessment for a particular bed using the electrofishing-video technique require more detailed costing taking into account factors such as the extent of the bed, distance from survey vessel home port and so on.

In addition, some areas for further development and testing of the technique are suggested.

Materials and Methods

Equipment

The surveys were conducted using commercial electrofishing gear on board the vessel ‘Lizanna’ (formerly ‘Nicola Jane’) operating out of Barra in the Outer Hebrides. The electrofishing equipment was the same as used by Marine Scotland in earlier trials on this vessel. The electrofishing equipment is fully described in Murray et al. 2014. Briefly the fishing rig consists of a series of copper electrodes fitted to an insulated supporting bar which is towed from the vessel - either in a tidal drift (paying out an anchored warp), or by ‘fly-dragging’ (towing towards an anchor), as illustrated below (Figure 1). During fishing alternating current is fed to the electrodes which results in electrical fields which stimulate razor clams to emerge from the sediment. The clams are then normally collected by a diver swimming along behind the rig.

Figure 1: Basic layout of the electrofishing rig (modified from Breen et al. (2011).

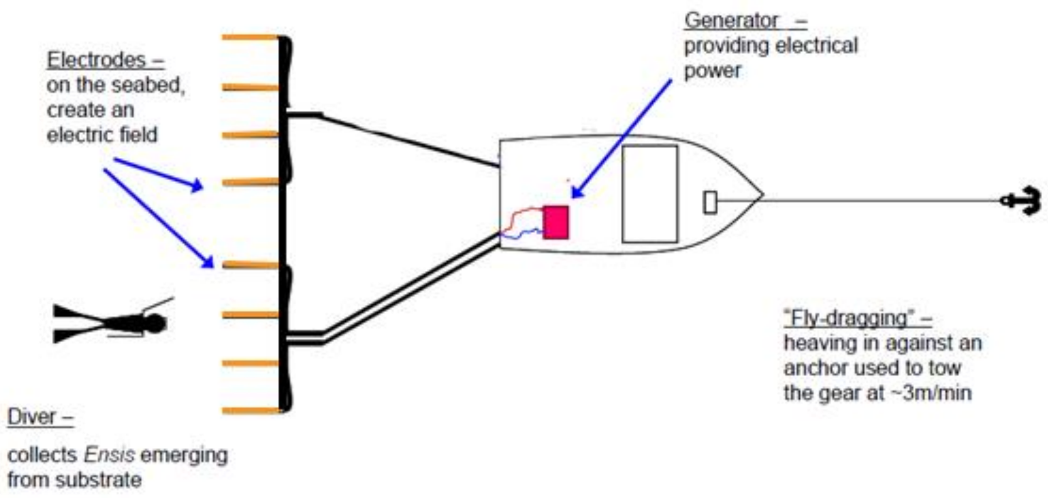

Three, downward-pointing Sony VN37CSHR cameras and a pair of downward-pointing 1 mW green-lasers (cruise 2 only) were mounted on a sled (Figure 2). The width between the sled shoes was 2 m and the cameras were mounted at a height of 68 cm. The cameras horizontal positions were adjusted so that the resulting images slightly overlapped resulting in a 1.5 m wide video swath as the sled was towed along the seabed.

Figure 2: The camera sled as setup during the first trip. At this stage it was unknown if there would be sufficient light for the video cameras on the seabed so the sled is shown fitted with two underwater (UW) lights. These turned out to be unnecessary and so were replaced with two vertically aligned laser pointers for the second trip (not shown).

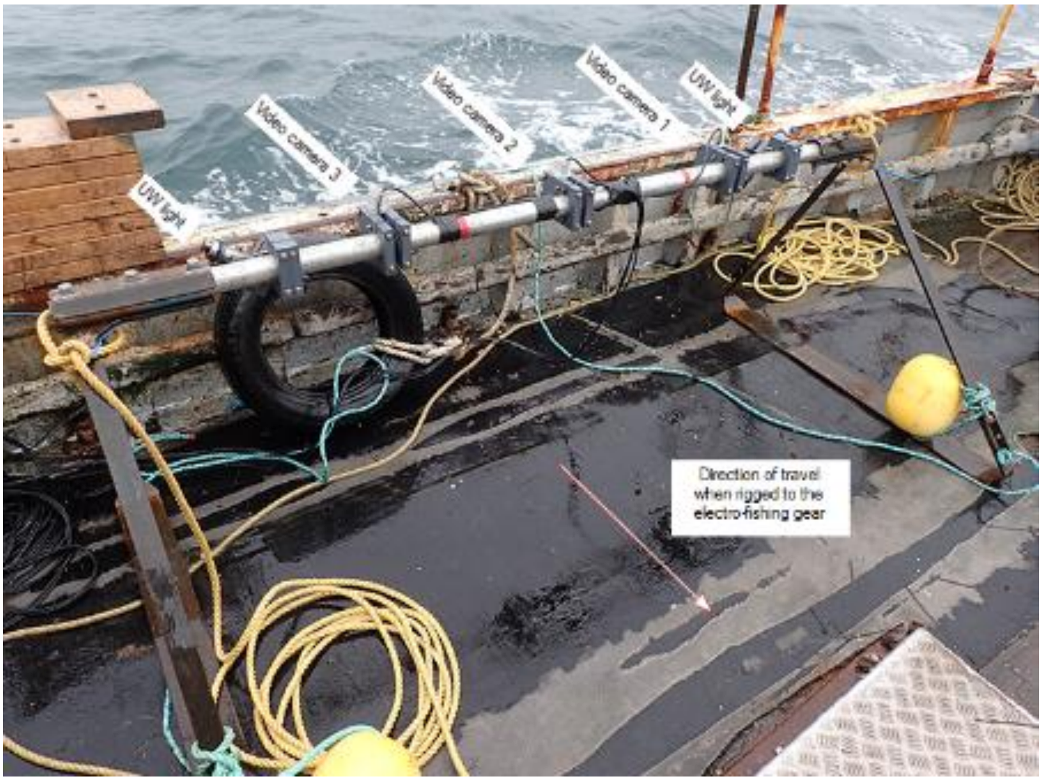

During fishing the camera sled was attached 2 m behind the electrode spreader bar by ropes. Power (12V DC) was fed to the cameras and lasers from the vessel by running additional cables down the main electrofishing power cable and the video feeds were captured on board the vessel using a digital video recorder (Hawk D1/960H AHD RF3089, RF Concepts, Belfast UK, *Figure 3*).

Figure 3: Setup of the recording DVR within the fishing vessel cabin.

Calibration of the Video Cameras

Prior to making measurements of objects from the video it was necessary to estimate and correct for camera lens distortion. An attempt was made to use the automated camera calibration tool in the Matlab Machine Vision Toolbox to estimate these parameters (MathWorks Inc., Natick, MA USA). However, that tool requires a checkerboard target to be imaged in varying three-dimensional orientations, which proved impractical underwater. The camera sled was therefore assembled and submerged in the seawater test-tank at the SAMS laboratory. A calibration target comprising three 44 cm white squares (internal dimensions) on a grey background was placed on the bottom of the tank and the overlapping images captured (Figure 4).

Figure 4: Still frames of the three calibration squares imaged in the SAMS test-tank. The images shown have not yet been corrected for camera lens-distortion. The green spots in the left and right-hand images are the distance-calibration lasers which were separated by a distance of 1.3 m.

An appropriate camera lens correction procedure was then estimated manually using a combination of fish-eye correction (Jaap de Vries' LensUndistort program) and image resizing in Matlab (see supplementary code sections of this report). This process resulted in three, distortion-corrected images which were then overlaid to form a composite of the total area imaged under the three separate video cameras (*Figure 5*). Slight distortions are still apparent, but only at the outer edges of the images.

Figure 5: The calibration squares after lens distortion correction, the three separate camera images (shown as green, white, purple) have been blended to show the composite of the original three-by-one calibration test squares.

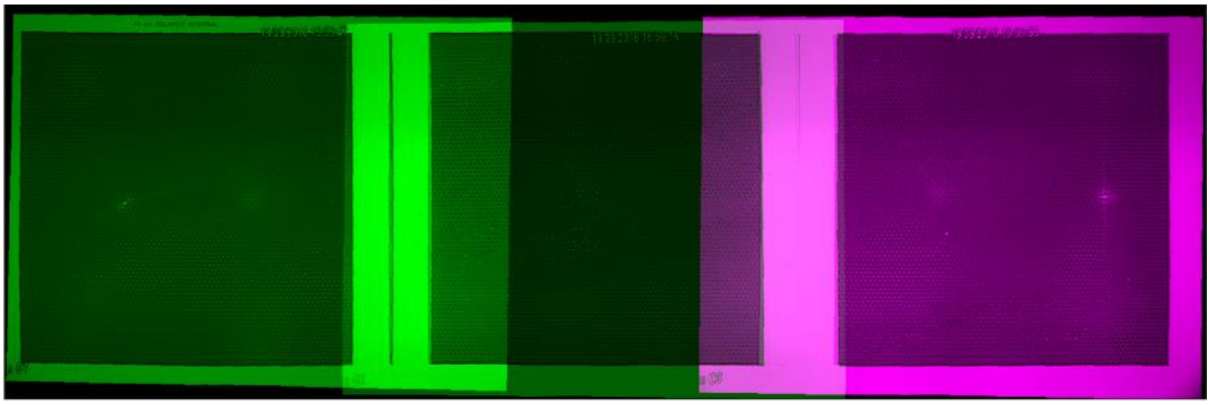

The final merged image is shown in (Figure 6). Each 44 cm calibration square has a side dimension of 410 pixels giving a pixel to real world conversion factor of 1 screen pixel = 1.0732 mm.

Figure 6: Final overlaying of the three distortion corrected images.

Additional inaccuracy due to the operator positioning the mouse in slightly different locations when recording length measurements on the computer screen was assessed by repeated measurements of a rectangle equivalent in length to 16 cm in the real-world (this is a typical length of a razor clam) using the Matlab ‘imtool’ measuring function (which was also used in the video analysis software). Length measurements ranged from 193 to 195 pixels, which equates to 2.5 mm in real world dimensions. Taking into account both the image distortion corrections and the ‘mouse position on screen’ variability, the length measurements of the razor clams collected from the video should be accurate to within +/- 2.5 mm. ‘Imtool’ also allows the operator to zoom the image allowing greater precision in placing the end-points of the length line, but this functionality was only used when measuring particularly small clams because it slowed down the measurement of objects on the video images.

Potential Impact on Video Estimated Lengths of Changes in Distance Between Camera and Target Object

Comparison of the test-tank image (Figure 6) with the real-world distance between the two laser-spots indicated that the accuracy of converting object lengths, when measured in pixels to real-world distances should be better than 1% (~1.3 cm error over the inter-laser separation distance of 1.3 m). Based on the laser calibration the length estimation error should be of the order +/- 0.75 mm for a razor clam of typical length 150 mm.

However, length conversions could also be affected by changes in the distance between the camera and the object being measured, for example if towing over a seabed with undulating sand-ripples. Imaging of a 150 mm target at different heights in the SAMS test-tank suggested that vertical displacements of 5 cm would cause a measurement error of around 1 cm (Figure 7).

Figure 7: Relationship between vertical displacements of the calibration block relative to the height of the cameras above the sled baseline (68 cm). The error is the calibration block length estimated from the video minus the actual calibration block length (15 cm). The solid line indicates a third-order polynomial fit, dashed lines are the 95% confidence intervals for the regression. Negative displacements >5 cm were not possible due to the depth of the test-tank.

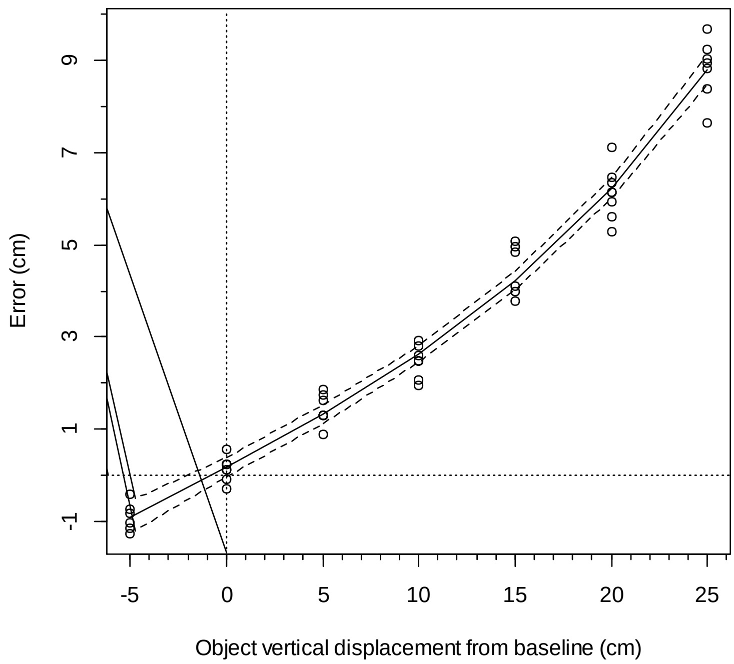

At the baseline setting the tank-based calibration indicated a slight positive bias in reconstructed lengths of about 2 mm (Table 3). It was not possible to make measurements of the undulations of the seabed in the field but large sand-ripples were not seen on the videos, or reported from the diver observations. An assumption was therefore made that vertical undulations between the sled-runners would be < 5 cm. These vertical displacements would include the thickness of the clam lying on its side. Reconstructed lengths of clams were thus expected to be accurate to within +/- 1.5 cm under these conditions.

Measurements of the widths of clams which were orientated vertically to the seabed would be substantially affected by how much of the shell had emerged. In these situations the shell tops were counted but not measured.

Table 3: Predicted errors when reconstructing the length of a 15 cm long calibration block from video with the object at different vertical displacements relative to the camera height on the sled.

Vertical displacement from sled baseline (cm)	Mean error (cm)	Lower 95% conf (cm)	Upper 95% conf (cm)
5	1.33	1.12	1.53
4	1.09	0.88	1.30
3	0.86	0.65	1.07
2	0.63	0.42	0.84
1	0.41	0.20	0.62
0	0.19	-0.02	0.39
-1	-0.03	-0.24	0.17
-2	-0.25	-0.46	-0.04
-3	-0.47	-0.70	-0.24
-4	-0.69	-0.97	-0.42
-5	-0.92	-1.26	-0.57

Processing the Videos

Captured video streams required a considerable amount of post-processing before measurements of the clams could be made so these steps were automated using a set of programs written in Matlab. The first program (Appendix 1) corrects the individual camera feeds for lens distortion and then combines the individual feeds to form a blended-image covering a swath with a real-world width of 1.5 m (Figure 6). It was originally hoped measurements could be directly taken from these blended images but, in some cases, timing synchronisation between the three cameras was not accurate enough. Each individual camera feed was therefore reproduced above the blended image, as shown in Figure 7. Combined frames were written out as a new video (one file per tow).

Figure 8: Still from video montage of the seabed as imaged by the three individual camera feeds. The individual distortion corrected images are shown in the top row and the merged image in the bottom row. All images are to the same scale so that object lengths can be collected from any of the images.

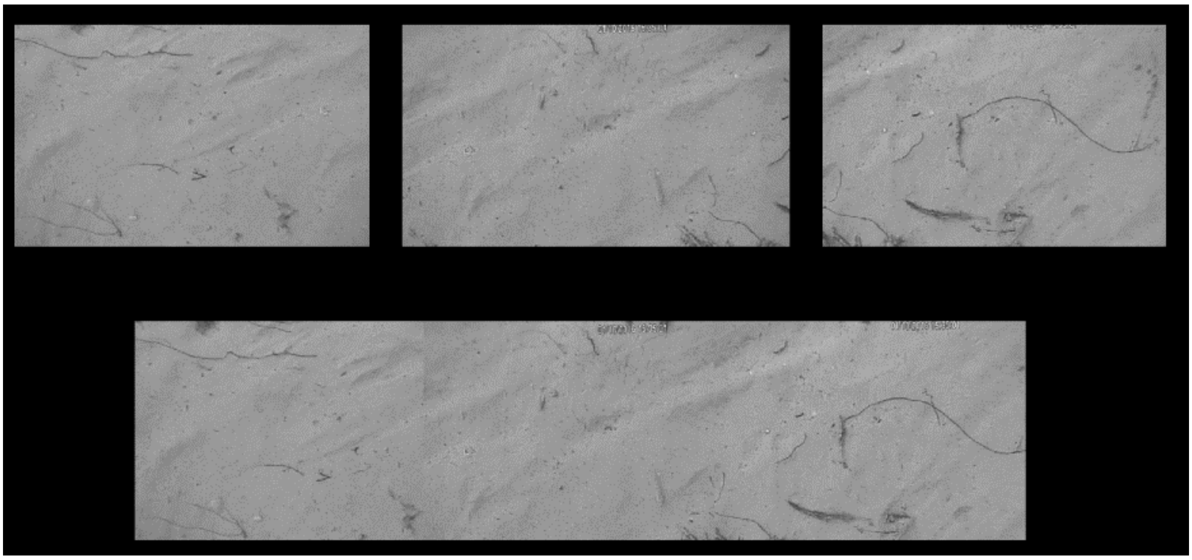

Counting and Estimation of Razor Clam Lengths from the Videos

A Matlab program was written to allow the lengths of objects to be inter-actively recorded from the merged-image videos (Figure 8).

Figure 9: The main control screen for the video objects measurement program.

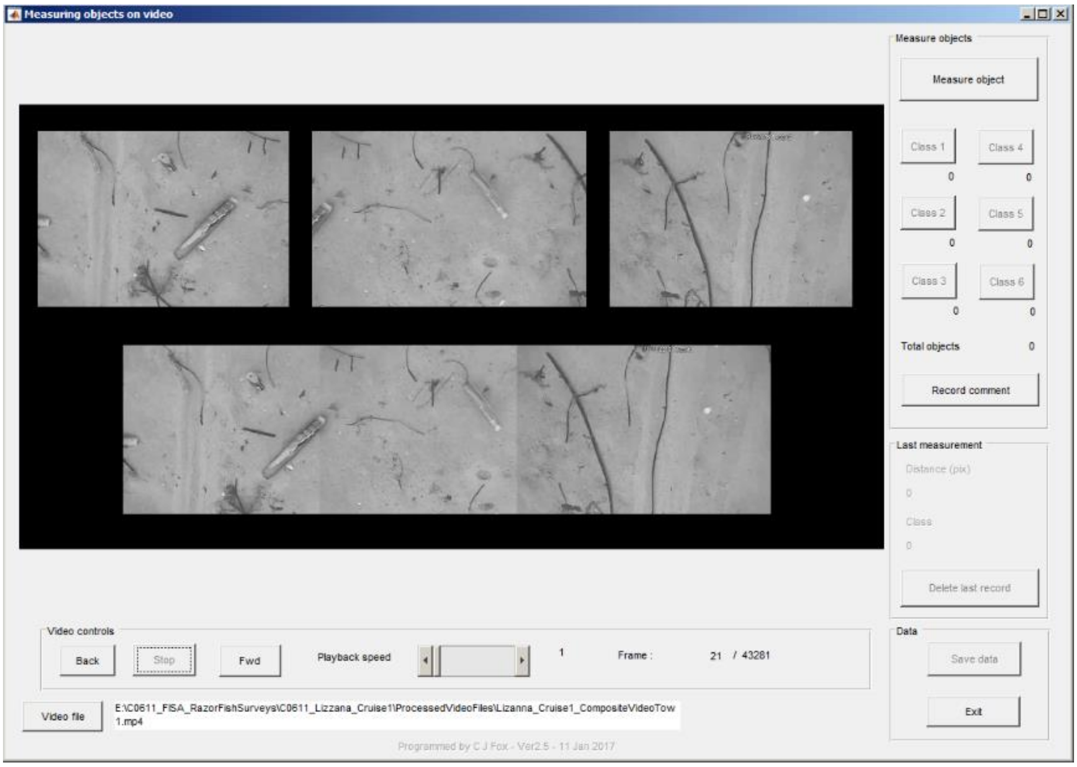

Further details of the program are provided in Appendix 3 but briefly the software allows the operator to play a video forward and back at varying speeds, to freeze the video at points of interest at which step a second, larger, measurement window opens (Figure 10).

Figure 10: The measurement screen of the video objects measurement program. The blue line is the length measurement tool which is overlaid by the operator on a small razor clam (upper middle image). Other clams are circled in red on lower composite image (circles have been added manually for illustrative purposes).

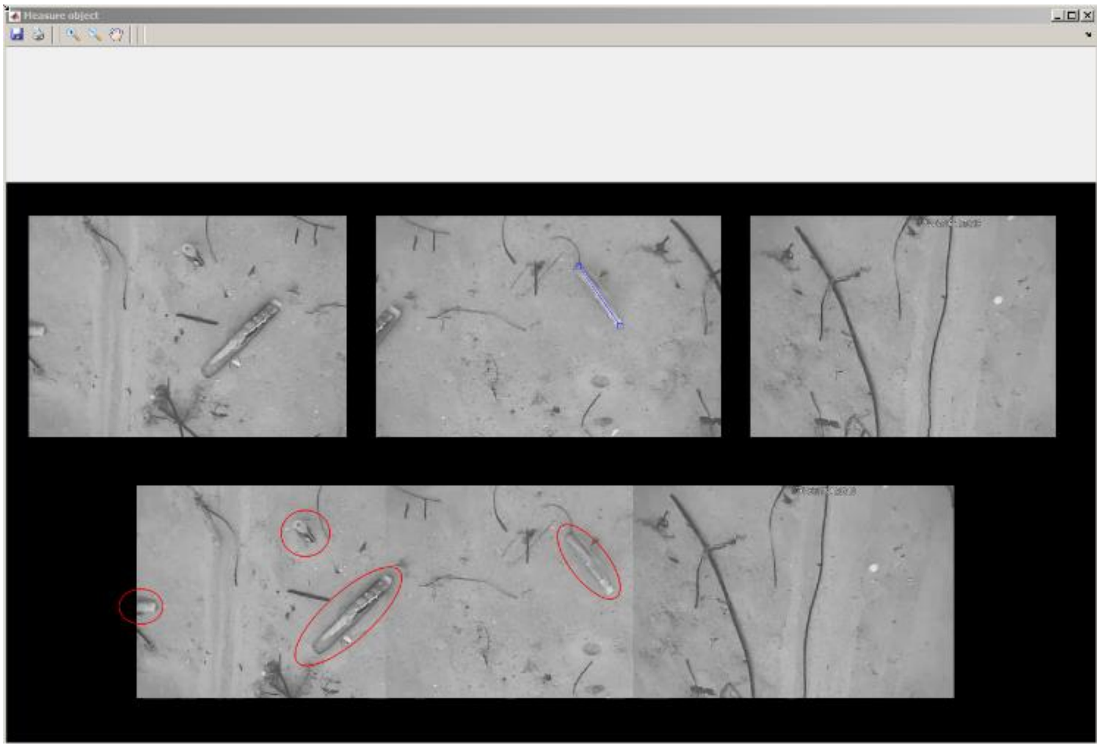

The lengths of objects (such as razor clams) are then recorded in pixels and assigned to one of 6 categories by the operator (Table 2).

Table 2: Categories used to record lengths of razor clams from the videos.

Category	Object
1	*E. siliqua* length when whole animal lying horizontally on the seabed
2	*E. siliqua* partial animal in view e.g. clam at edge of the camera frame
3	Width of razor clam if only top visible – this occurred for some individuals which had either not fully emerged or had partially re-buried, because the estimated real-world width will be affected by the height to which the clam emerged these data were subsequently treated as counts only
4	*E. arcuatus* length when whole animal lying horizontally on the seabed
5	*E. arcuatus* partial animal in view e.g. clam at edge of the camera frame
6	Un-used category

Along with the length measurements, the video frame number and elapsed video time where the object was measured are recorded by the software. In addition, short text comments can be recorded e.g. if the video became obscured at a certain point by macro-algae or seagrass.

Because the videos had previously been corrected for lens distortion the relationship between pixel distance and real-world distance was known, allowing the length measurements recorded in pixels to be converted to millimetres.

Estimation of the Length of the Tows

The start and end positions of tows were recorded from the ship's plotter (GPS) and used to estimate the length of the tows (Table 3). However, this approach might result in some inaccuracies because the position of the vessel, relative to the camera rig, varied between the starts and ends of tows due to changes in tide and wind. In addition, we were interested in examining how the clams were distributed along the tow tracks because this information was needed to address questions around survey design. Video frame numbers were converted to distance by vertically stitching the video from one of the camera feeds using automatic feature recognition and alignment tools available in the Matlab Computer Imaging toolbox (see Appendix 2 for code). Because the video images had been calibrated to real world measurements the resulting vertically stitched image could be used to produce a relationship between video frame number and distance travelled along the tow track. Although stationary objects, such as seabed features, are correctly rendered in the resulting image it was not possible to measure the sizes of razor clams on the vertically stitched images. Many of the clams moved using foot-kicks between successive video frames and this caused shape distortion in the vertical stitching process (Figure 11). Although the moving object will be identified as a feature by the montaging process, a statistical sub-setting is used to weight the image frame shift and there were normally enough stationary features identified so that moving objects were ignored by the algorithm. The software skips any image pairs where there are insufficient matched features to calculate the vertical shift between frames.

Figure 11: Section of vertically stitched tow. Whilst the seabed appears to be correctly blended some of the clams appear elongated due to their movement between successive video frames. The grey ticks down the edge of the track indicate stitched frames, the short white ticks indicate 0.5 m distance marks and the longer white ticks, 1 m distance marks.

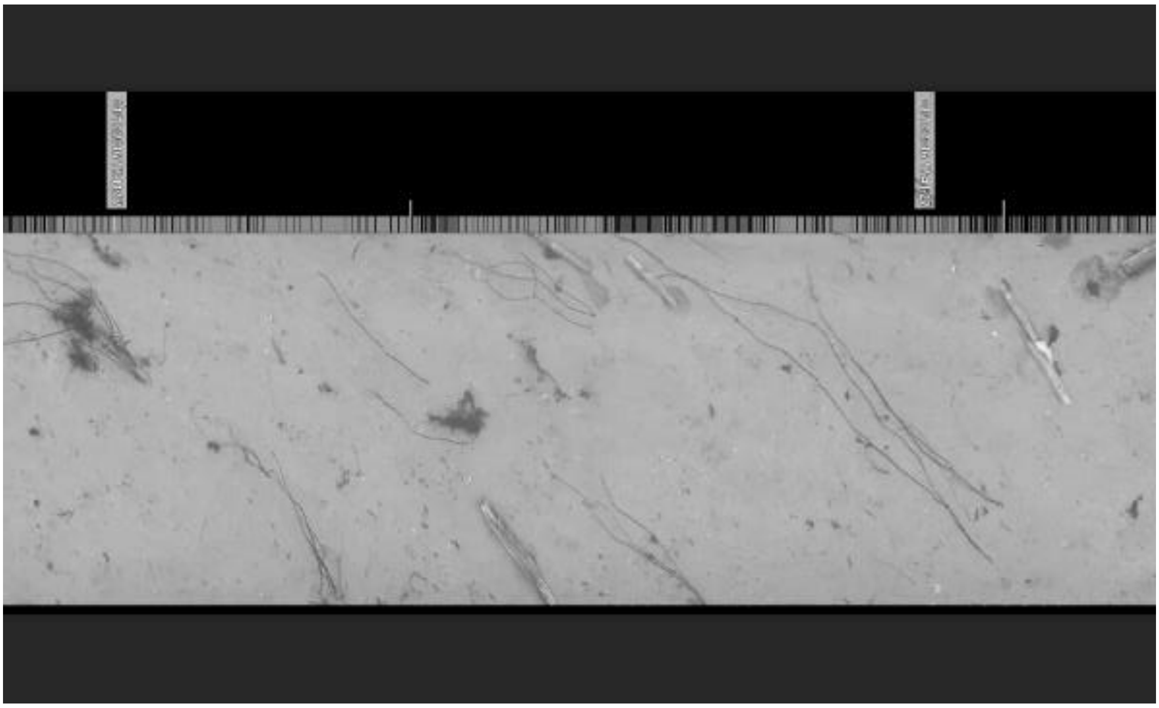

Surveys

All the fishing surveys described here were undertaken under fisheries research derogations granted by Marine Scotland (Fisheries Compliance). Video surveys were conducted at three locations (Figure 12): the first trip on the 9th and 10th August 2016 worked to the south (Figure 13) and southeast (Figure 14) of the Isle of Fuday; due to deteriorating weather the second trip on 1st and 2nd October 2016 was split between the southeast of Fuday (Figure 15) and the more sheltered Sound of Eriskay (Figure 16).

Figure 12: Start locations of all the tows made. Underlying chart © SeaZone Solutions, 2013.

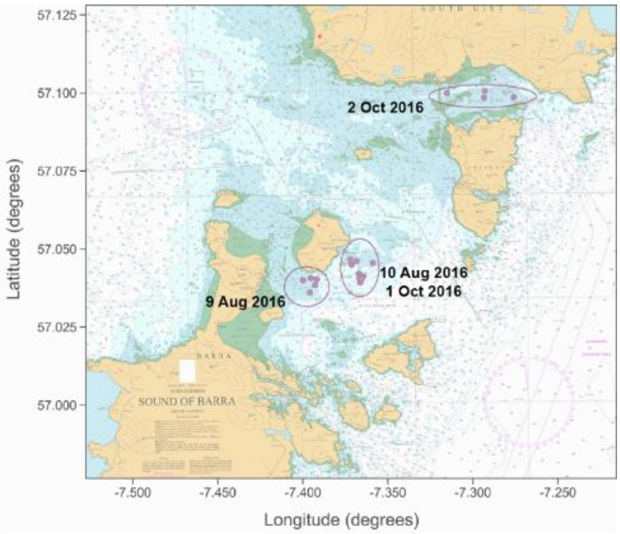

Figure 13: Detail of tows undertaken on 9th Aug 2016 (Trip 1). Underlying chart © SeaZone Solutions, 2013.

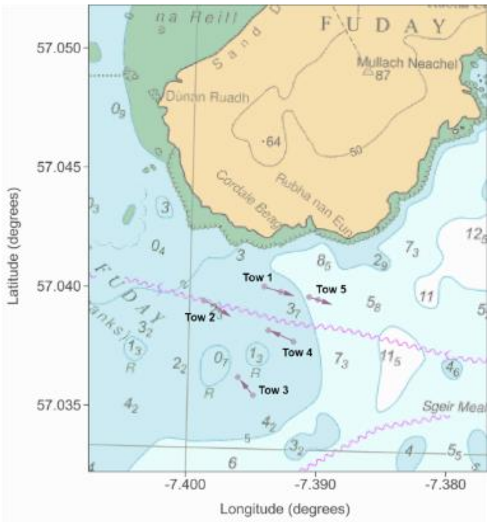

Figure 14: Detail of tows undertaken on 10th Aug 2016 (Trip 1). Underlying chart © SeaZone Solutions, 2013.

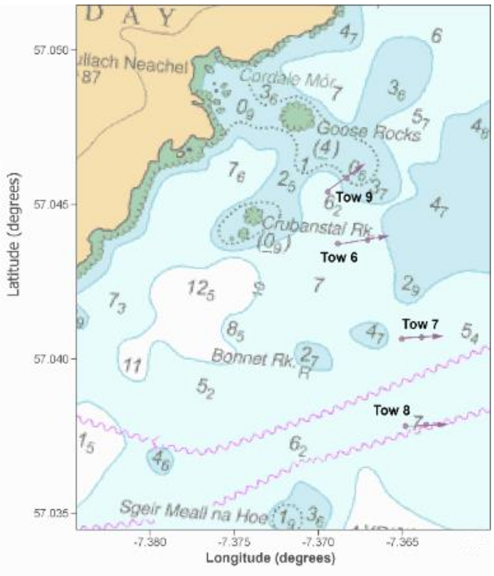

Figure 15: Detail of tows undertaken on 1st Oct 2016 (Trip 2). Underlying chart © SeaZone Solutions, 2013.

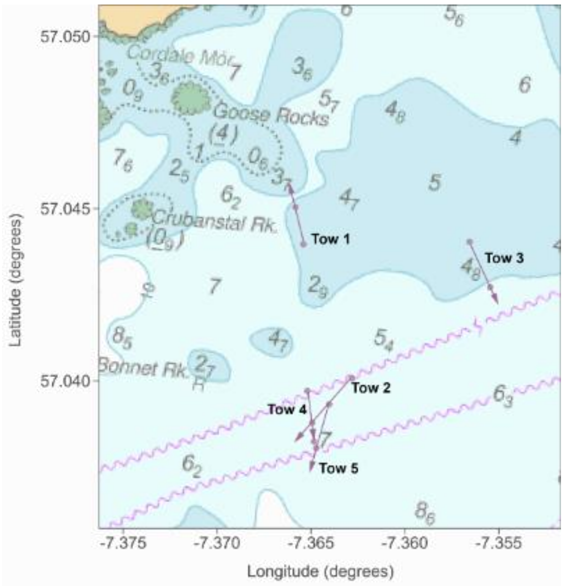

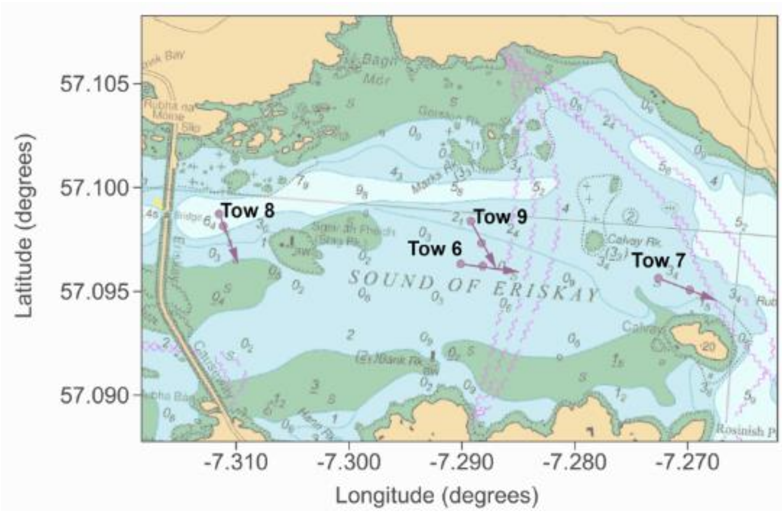

Figure 16: Detail of tows undertaken on 2nd Oct 2016 (Trip 2). Pink circles indicate start and end locations, arrow is direction of travel. Underlying chart © SeaZone Solutions, 2013.

The location and direction of tows was selected by the skipper based on his experience and the tidal conditions. Because this was a pilot study it was not practical to apply a full statistical survey design at this stage but the sampling allowed a number of replicated tows within each area. In addition, the tows covered a range of depths (5-12 m) and bottom conditions, from clean sand to areas with patches of seagrass and/or macro-algae.

At the start of each tow the electrofishing gear was dropped to the seabed and the electrodes laid out (Figure 17). The camera sled was then lowered into place and attached to the non-conducting electrode bar. Both of these steps had to be undertaken by a diver. The electrodes and cameras were then turned on and, once it was confirmed on-board that everything was working, the diver returned to the vessel.

Tows lasted between 32-64 minutes and were estimated to cover up to 190 m (Table 3). At the end of each tow the equipment was recovered and the vessel moved to the next start. Water temperature and salinity were recorded at least once a day using a Castaway CTD (SonTek Ltd., San Diego, USA).

Figure 17: The electrofishing rig and camera rig being manoeuvred into their towing positions at the start of a tow. Once the electrofishing rig was laid out correctly, the camera rig was moved into position centrally behind the electrode spreader bar and attached with two, 2 m long ropes to the spreader.

Measurement of Sampled Animals

On one tow at each site the diver stayed in the water and collected emerging razor shells for around 10 minutes so that these animals could be measured on-board and compared to the lengths estimated from the video. After the animals had been separated into *E. siliqua* and *E. arcuatus* on the basis of their shapes, their lengths were recorded to the nearest millimetre using a fish measuring board (Figure 17).

Figure 18: Measuring a sample of razor clams on board the fishing vessel.

Table 3: Tow details.

Trip	Tow	Date	Site	Tow start Time (UTC)	Tow start Position (dec deg)	Tow end Time (UTC)	Tow end Position (dec deg)	Depth (m)	Tow dur (mins)	Tow len[b] (m)	Tow len[c] (m)	Swept area (m^2)	CTD	Notes
1	1	9 Aug	S Fuday	11:00	57.040 -7.394	11:34	57.040 -7.393	12	34	79.8	73.6	110.4	Yes	
	2	9 Aug		12:15	57.040 -7.399	13:05	57.039 -7.398	7	50	81.5	79.6	119.4		Clam samples collected
	3	9 Aug		13:46	57.036 -7.395	14:21	57.036 -7.396	7	35	108.5	110.0	165		
	4	9 Aug		15:15	57.038 -7.392	15:56	57.038 -7.394	6	41	128.1	120.8	181.2		
	5	9 Aug		16:30	57.040 -7.391	16:52	57.040 -7.390	9	22	42.8	58.2	87.3		Weedy
	6	10 Aug	SE Fuday	10:13	57.044 -7.370	11:00	57.045 -7.368	11	47	109.2	103.7	155.6	Yes	
	7	10 Aug		11:43	57.041 -7.366	12:30	57.042 -7.365	11	47	71.4	64.9	97.4		Clam samples collected
	8	10 Aug		13:09	57.039 -7.365	13:42	57.039 -7.364	11	33	74.4	72.3	108.5		Wind freshening
	9	10 Aug		14:30	57.046 -7.371	15:02	57.047 -7.370	10	32	85.2	70.9	83.7	Yes	Camera 2 failed[d]
2	1	1 Oct	SE Fuday	10:27	57.046 -7.367	11:25	57.044 -7.367	8	58	123.5	141.7	212.6	Yes	Strong current, weedy
	2	1 Oct		12:09	57.041 -7.363	13:08	57.039 -7.365	10	59	193.8	187.4	281.1		
	3	1 Oct		14:00	57.045 -7.358	14:55	57.044 -7.356	8	55	160.8	143.8	215.7		
	4	1 Oct		15:35	57.040 -7.366	16:39	57.039 -7.366	12	64	164.8	152.7	229.1		
	5	1 Oct		17:17	57.040 -7.365	18:10	57.039 -7.365	12	53	147.7	148.9	223.4		
	6	2 Oct	Snd Eriskay	07:35	57.098 -7.291	08:33	57.098 -7.289	6	58	118.8	119.1	178.7		Thick seagrass patches
	7	2 Oct		09:07	57.098 -7.274	10:08	57.097 -7.271	6	59	179.3	-[e]	269.0		Clam samples collected
	8	2 Oct		11:05	57.099 -7.313	11:38	57.098 -7.313	11	33	68.6	73.3	110.0	Yes	Cluttered seabed
	9	2 Oct		12:20	57.010 -7.290	13:08	57.099 -7.290	5	48	131.1	115.9	174.9		Wind strengthened too much to work further

[b] Calculated from vessel start and end latitude, longitude positions using Haversine formula with mean earth radius set at 6,371 km.

[c] Estimated from vertical montage for camera 1 from each tow

[d] The swath width and swept area estimates were corrected for the camera failure on this tow

[e] It was not possible to vertically montage this video because of silt stirred up by the diver whilst collecting live clam samples. Stitching also failed towards the end of the tow due to a lack of seabed features.

Results

Temperature and Salinity

There were virtually no changes in temperature or salinity with depth due to the shallow depths sampled and the degree of wind and tidal mixing. Table 4 therefore shows depth averaged values for these parameters. There was very little difference in water temperature, and none in salinity, between the two trips.

Table 4: Depth averaged water column temperature and salinity.

Trip	Date	Site	Time (UTC)	Lat (Dec deg)	Lon (Dec deg)	Temp (^oC)	Salinity
1	9 Aug	S Fuday	11:56	57.040	-7.400	13.8	34.4
	9 Aug		13:08	57.040	-7.397	13.7	34.4
	9 Aug		16:07	57.038	-7.394	13.5	34.4
	10 Aug	SE Fuday	11:29	57.042	-7.367	13.3	34.5
	10 Aug		12:33	57.042	-7.365	13.3	34.4
	10 Aug		15:06	57.047	-7.370	13.3	34.4
	10 Aug		16:50	57.045	-7.368	13.2	34.4
2	1 Oct	SE Fuday	11:06	57.045	-7.367	13.0	34.4
	2 Oct	Snd Eriskay	11:28	57.100	-7.313	12.8	34.4

Sampling and Video Quality

A total of 18 tows were completed over three sites (Figure 12) with tows being between 32-64 mins duration (Table 3). Recovery and setting up of the gear for each tow proved to be quite time-consuming so that most tows were separated by at least 30 minutes. This form of fishing also requires calm weather which deteriorated towards the end of both trips. This was particularly the case on the second trip and resulted in some of the tows planned for the afternoon of 2nd October having to be abandoned.

Based on the vessel start and end positions total tow distances were estimated at between 43 and 194 m. As judged from the final stitched images automated vertical stitching appeared to work well on most videos with congruence of seabed features being visible throughout the majority of each tow (Figure 19). An exception was tow 7 of trip 2 which could not be vertically stitched because of sediment stirred up by the diver collecting live samples combined with a strong tidal flow obscuring the seabed features. There was also a lack of clear seabed features towards the end of this particular tow. For that tow the estimate of tow length was based on the geographic co-ordinates. The estimated total tow distances based on vertically stitched videos were between 58 and 187 m (Table 3). Overall there was good agreement between the geographic-based and video-based estimates of total tow length (correlation coefficient 0.972) with an overall difference of +1.3% (std dev 11.7%, n=17).

Figure 19: Part of the vertically stitched video for Trip 1, Tow 1. Stitching appeared generally good with problems in pattern matching only occurring where multiple objects moved between frames. The grey blocks down the left edge of the track indicate stitched frames, the short white ticks indicate 0.5 m distance marks and the longer white ticks, 1 m distance marks.

The results from the vertical stitching were used to estimate the total swept areas (except for trip 2 tow 7) because this also allowed the locations of measured objects (clams) to be related to distance along the tow tracks (Figures 20 and 21). Based on the vertical stitching results, the average speeds of the electrofishing/camera rig over the ground were estimated to vary between 1.2 and 3.2 ms^{-1}.

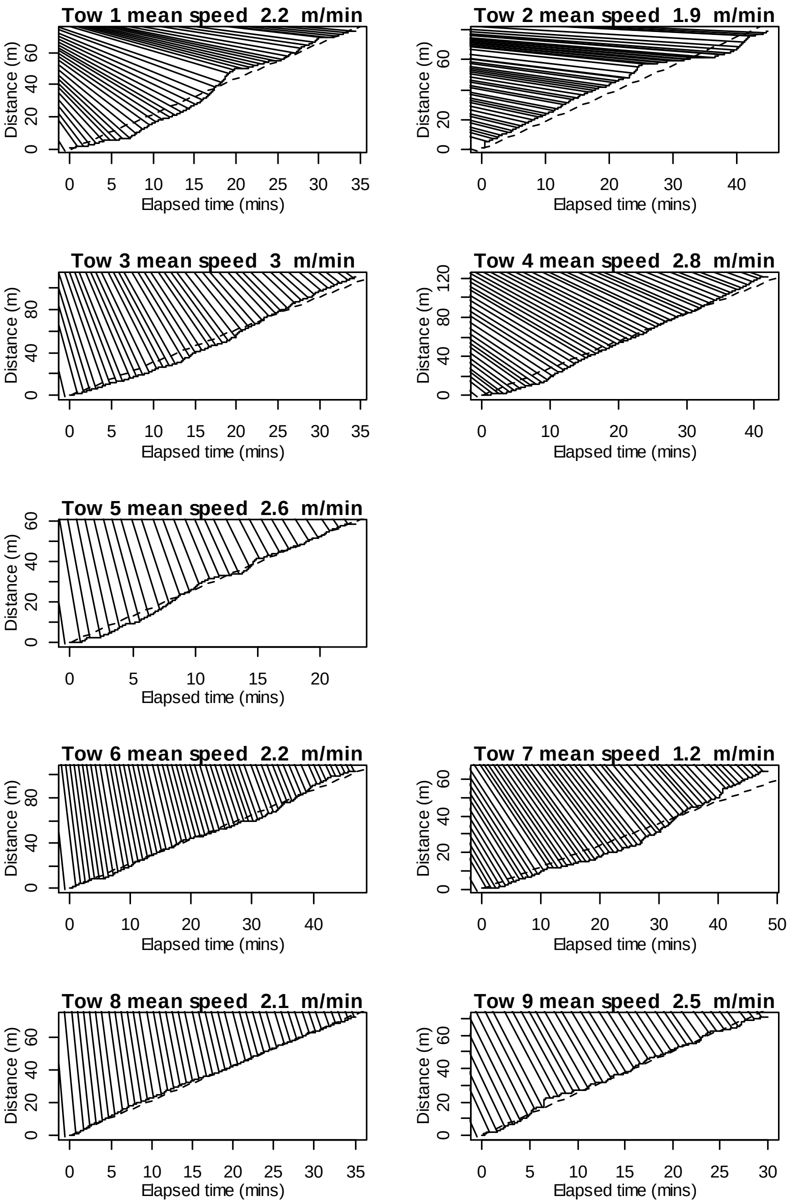

Figure 20: Video-based estimates of the relation between elapsed time and tow distance for trip 1. The actual estimate of distance versus time is shown by the solid line while the dashed line shows the average speed as fitted by linear regression.

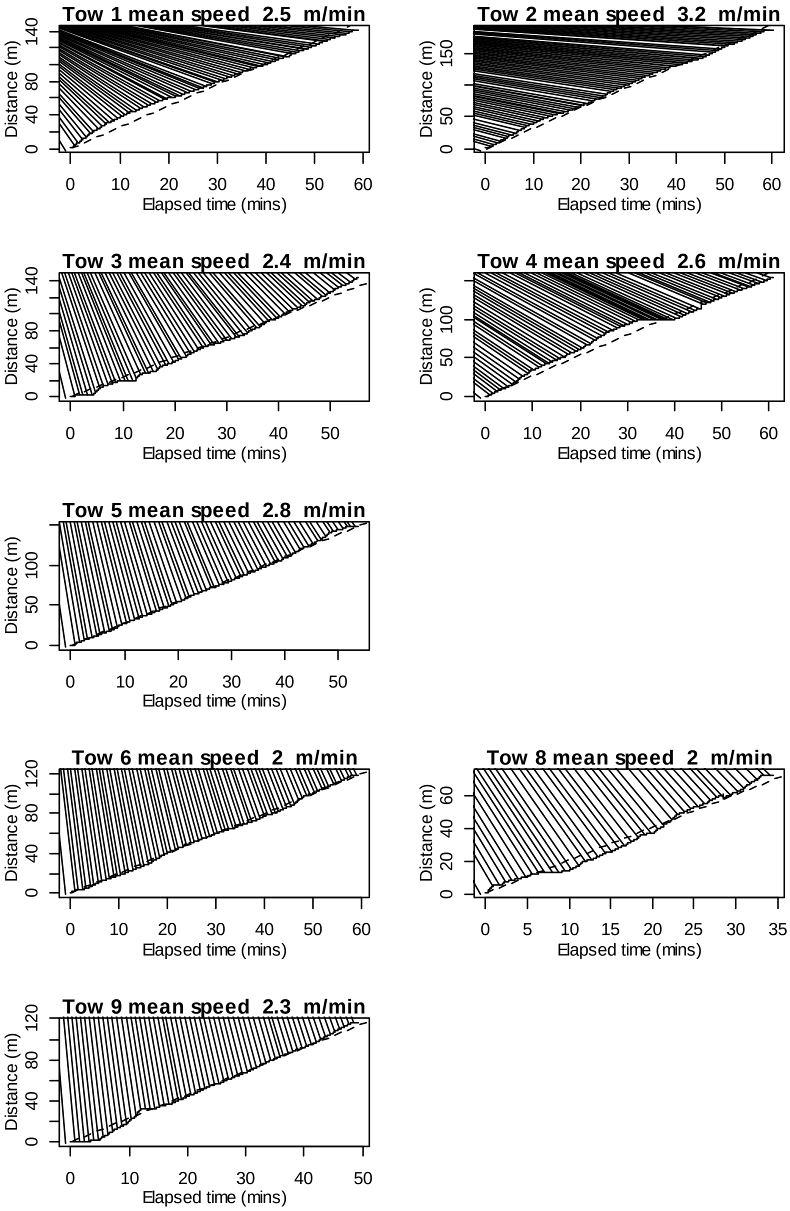

Figure 21: Video-based estimates of the relation between elapsed time and tow distance for trip 2. The actual estimate of distance versus time is shown by the solid line while the dashed line shows the average speed as fitted by linear regression.

The quality of the video obtained was generally good with the cameras adjusting automatically to the varying light levels at different depths. Razor clams, as well as other benthic organisms could be easily seen on the videos (Figure 23). The most common non-target benthic organisms seen in the video were crabs (Table 5), the majority of which appeared to be shore crabs (*Carcinus maenas*), although a few spider crabs (not identified to species) were also seen. Crabs were often mobile but only two shore crabs were observed actively predating on stunned razor clams (Trip 1, Tow 2; Trip 2 Tow 7). Small sandeels and flatfish were also seen, but in low numbers.

Figure 22: Target and non-target benthic organisms seen in video collected to the south of Fuday (Trip 1, tow 1).

Top image: A small flatfish (possibly a dab) seen swimming across the field of view while two razor clams are lying to the left.

Lower image: A moribund sandeel lying on the sediment surface. A clam is lying partially across the image boundary to the left.

Table 5: Counts of non-target benthic organisms by tow.

Trip	Tow	Crab	Sand -eel	Flat- fish	Other fish[f]	Star- fish	Scallop	Butter - fish	Shrimp	Other bivalve
1	1	6	3	2	-	-	-	-	-	-
	2	16	1	4	4	-	-	-	-	1
	3	27	-	-	1	-	-	1	-	1
	4	10	5	-	-	-	-	-	-	-
	5	1	-	-	-	-	-	-	-	-
	6	24	3	1	-	-	-	-	-	-
	7	9	1	1	-	-	-	-	-	-
	8	10	1	-	-	-	-	-	-	-
	9	16	-	1	-	-	-	-	-	-
2	1	17	-	-	1	-	-	-	-	-
	2	29	7	-	-	3	-	-	-	-
	3	13	6	2	1	-	-	-	-	-
	4	32	7	7	-	2	-	-	-	-
	5	41	5	10	-	-	-	-	1	-
	6	15	-	-	3	-	-	-	-	-
	7	24	-	3	-	-	-	-	-	-
	8	25	-	-	1	1	4	-	-	-
	9	3	1	2	3	1	-	-	-	-
Total		318	40	33	14	7	4	1	1	2

[f] Majority appeared to be gobies

There were some areas where seagrass or macro-algae obscured the camera view (Figure 23). Even on these patches clams could usually be counted, even if their lengths could not be recorded.

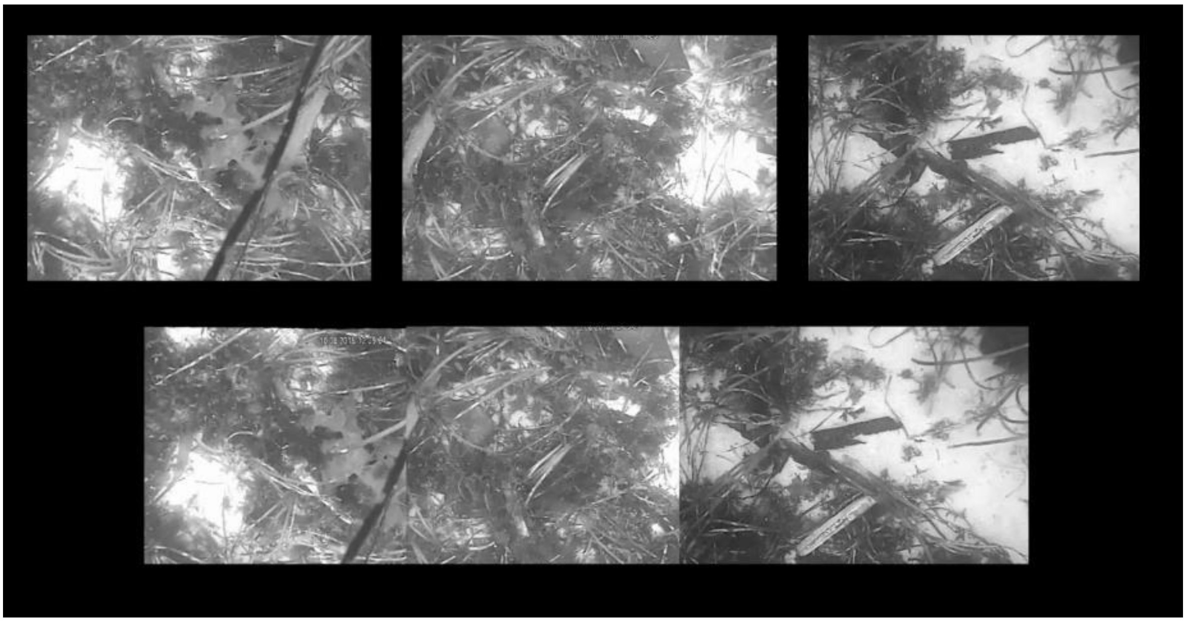

Figure 23: Obscured area of video (Trip 1, Tow 7)

The majority of razor clams were observed lying stationary on the seabed (Figure 22) but active individuals were also seen moving by foot-kicking, and, in some cases, were observed recovering to a vertical position and re-burying. Active clams sometimes swan into or out of the field-of-view so care was taken not to double-count these animals. It was usually obvious when a razor clam was dead because the two shell valves had separated, or there was a lack of any white muscle visible at the shell border. Few obviously dead clams were seen apart from one tow in the Sound of Eriskay (tow 8) which was particularly cluttered with large numbers of apparently dead shells (Figure 24). The numbers of razor clams measured and counted from the videos are shown in Table 6 (Trip 1) and Table 7 (Trip 2).

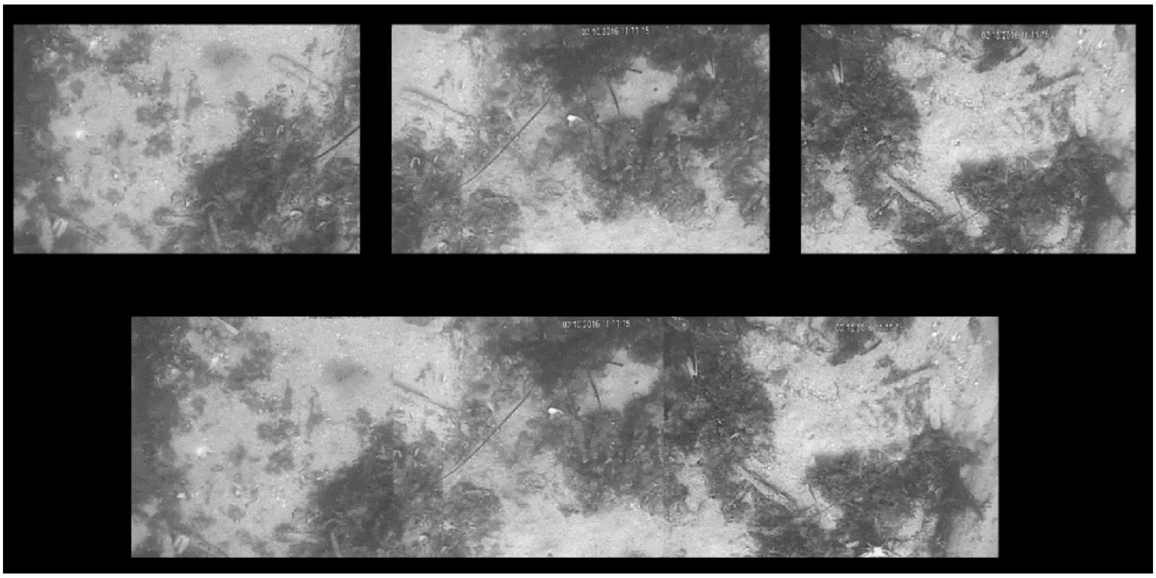

Figure 24: Cluttered seabed with a number of apparently dead razor clam shells near the causeway in Sound of Eriskay (Trip 2, Tow 8).

Table 6: Numbers of Ensis razor clams counted and measured* from Trip 1 videos.

Category		Tows S Fuday					Tows SE Fuday				Total
		1	2	3	4	5	6	7	8	9	
1	Whole *siliqua**	178	124	231	343	61	261	217	298	129	1842
2	Part *siliqua*	20	17	37	33	15	35	49	58	30	294
3	Tops[g]	23	19	25	32	17	40	44	65	28	293
4	Whole *arcuatus**	14	11	25	28	6	16	10	21	12	143
5	Part *arcuatus*	1	0	0	2	0	0	2	1	0	6
Total		236	171	318	438	99	352	322	443	199	2578
Swept area (m^2)		110.4	119.4	165	181.2	87.3	155.6	97.4	108.5	83.7	
Density (nos m^{-2})	*E. siliqua*	1.70	1.11	1.51	1.98	0.78	1.79	2.48	3.01	1.72	
Density (nos m^{-2})	*E. arcuatus*	0.13	0.09	0.15	0.16	0.07	0.10	0.11	0.20	0.14	

Table 7: Numbers of Ensis razor clams counted and measured* from Trip 2 videos.

Category		Tows SE Fuday					Tows Sound of Eriskay				Total
		1	2	3	4	5	6	7	8	9	
1	Whole *siliqua**	202	644	141	666	574	320	461	16	152	3176
2	Part *siliqua*	27	77	23	53	43	27	48	1	18	317
3	Tops[h]	21	66	17	99	108	22	24	11	27	395
4	Whole *arcuatus**	8	39	7	35	36	17	17	98	38	295
5	Part *arcuatus*	0	2	0	1	0	1	0	9	1	14
Total		258	828	188	854	761	387	550	135	236	4197
Swept area (m^2)		212.6	281.1	215.7	229.1	223.4	178.7	269	110	174.9	
Density (nos m^{-2})	*E. siliqua*	1.01	2.43	0.71	3.02	2.67	1.87	1.80	0.15	0.92	
Density (nos m^{-2})	*E. arcuatus*	0.04	0.14	0.03	0.15	0.16	0.10	0.06	0.93	0.22	

[g] Where only the top of the clam was visible these were assumed to be *E. siliqua*

[h] Where only the top of the clam was visible these were assumed to be *E. siliqua*

Size Frequencies of the Razor Clams - Comparison of Lengths Estimated from the Videos with Lengths Measured on Live *Ensis*

Shell lengths of whole *E. siliqua* estimated from the videos are compared with measurements on live samples in Figure 25. The live sample for trip 1, tow 2 (9th Aug) clearly only contained larger 'commercial-size' shells. Following this the diver was asked to collect all sizes of shells from subsequent comparison tows. Comparing the video and live-based data the range of shell sizes in the latter two tows, as well as the locations of the modes, appear similar (at least to within 1 cm), although relatively more small individuals were observed on the video. For the latter two tows, Kolmogorov-Smirnov tests failed to reject the null hypothesis that the samples were drawn from the same distribution (10 Aug, Tow 7; D = 0.13, p-value = 0.12; 2 Oct, Tow 7; D=0.10, p-value=0.26).

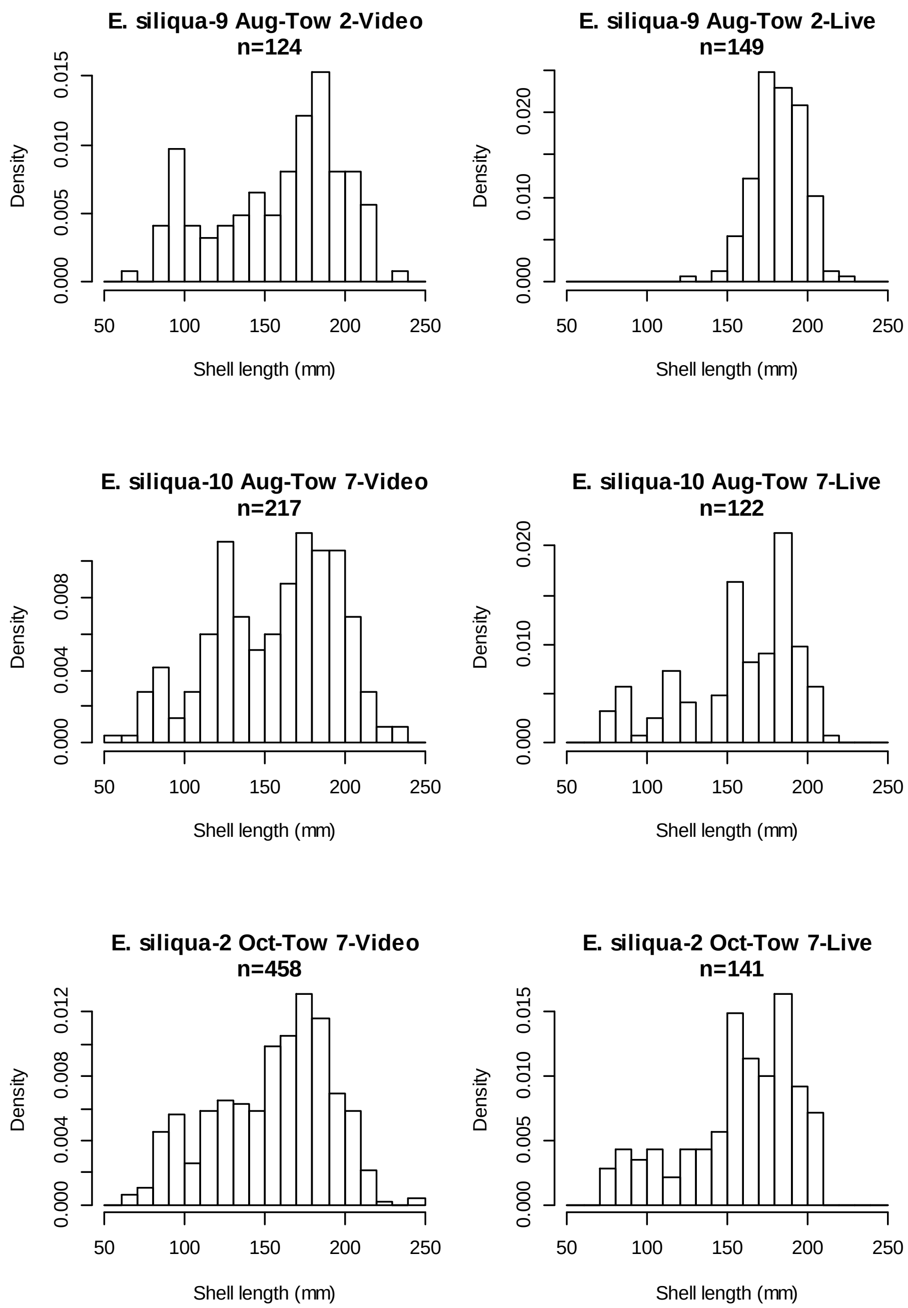

Figure 25: Comparison of size frequencies of *E. siliqua* as measured from towed video and from the live samples collected by the diver during the video tows.

Many fewer clams were assigned as *E. arcuatus* on the videos and there were also many fewer of this species in the live samples. It was therefore reassuring that *E. arcuatus* did not appear to be abundant in the live samples where the differences in shell curvature are more obvious. The total numbers of live *E. arcuatus* samples were too low for meaningful statistical comparisons of the video-estimated and live lengths but the plots are shown for completeness (Figure 26). Again the modal lengths for video and live samples appear to be in reasonable agreement.

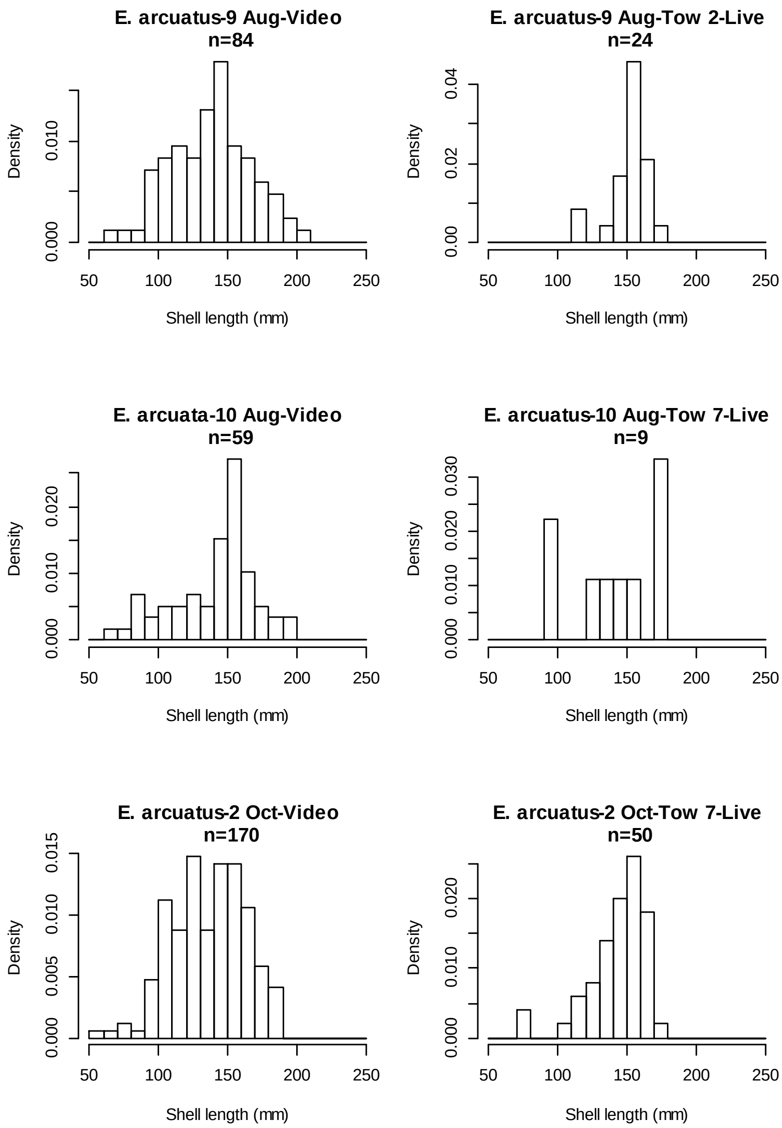

Figure 26: Comparison of size frequencies of *E. arcuatus* as measured from towed video and from the live samples collected by the diver during the video tows.

The limited comparisons of video-based lengths with live-lengths undertaken in the present study thus gave no reason to suspect that the video-based length measurements were substantially biased. Further testing of the accuracy and precision of video-based length estimation is however recommended if the electro-fishing video technique were to be deployed more widely for stock assessments, particularly in areas with an undulating seabed.

Size Frequencies of the Razor Clams in the Different Sampling Areas and Tows

E. siliqua length frequencies pooled by site (Figure 27) suggested that the populations were comprised of two, or perhaps three size groups, the modes being at about 85, 125 and 170 mm. Except for tows conducted on 1st October to the SE of Fuday the populations were dominated by larger clams. However, video from earlier tows at this site (10th Aug) had contained more, larger animals.

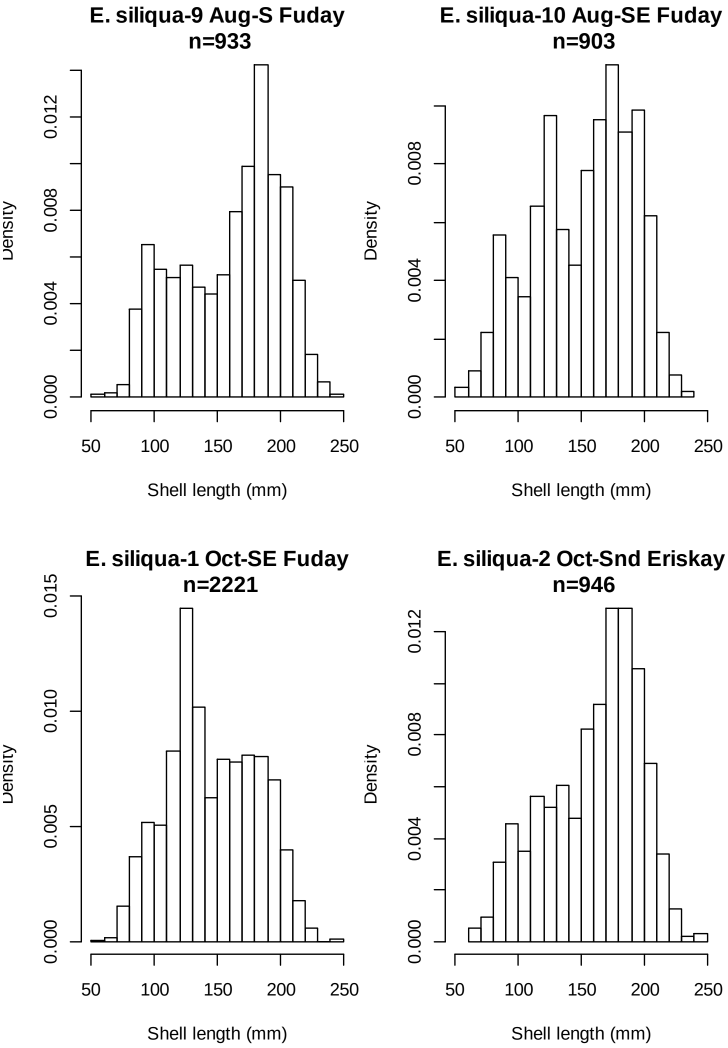

Figure 27: Size frequencies of shell lengths of whole *E. siliqua* measured from towed video collected on 9 August, S of Fuday (top left); 10 August, SE of Fuday (top right); 1 October, SE of Fuday (bottom left) and 2 October, Sound of Eriskay (bottom right).

The frequency of each length class is shown as a proportion so that the distributions across sites can be compared even though different numbers of clams were measured.

Most of the length frequency plots from the separate tows conducted in each site were reasonably similar to each other (Figures 28-31). An exception was Tow 8 in the Sound of Eriskay (Figure 31) which had a much lower abundance of *E. siliqua* than for the tows further to the east. This was related to the coarser sediment at this location. Large numbers of dead shells were also observed on this tow (Figure 24).

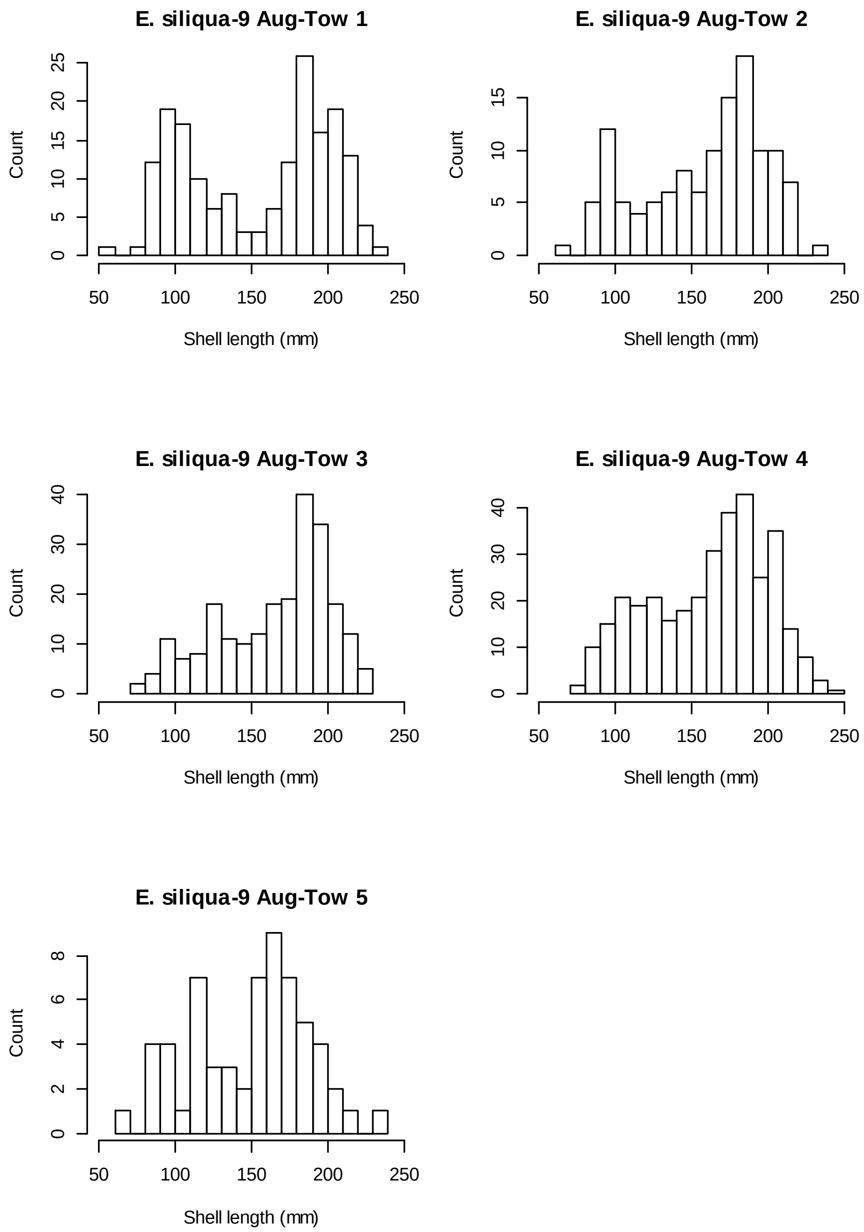

Figure 28: Size frequencies of shell lengths of whole *E. siliqua* measured from towed videos collected on 9th Aug, S of Fuday.

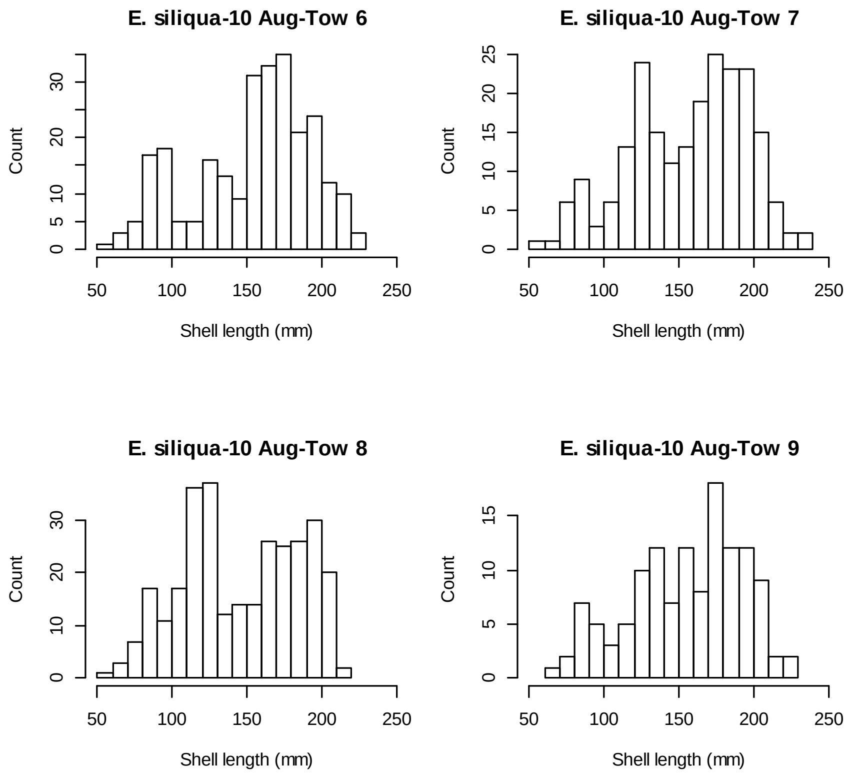

Figure 29: Size frequencies of shell lengths of whole *E. siliqua* measured from towed videos collected on 10th Aug, SE of Fuday.

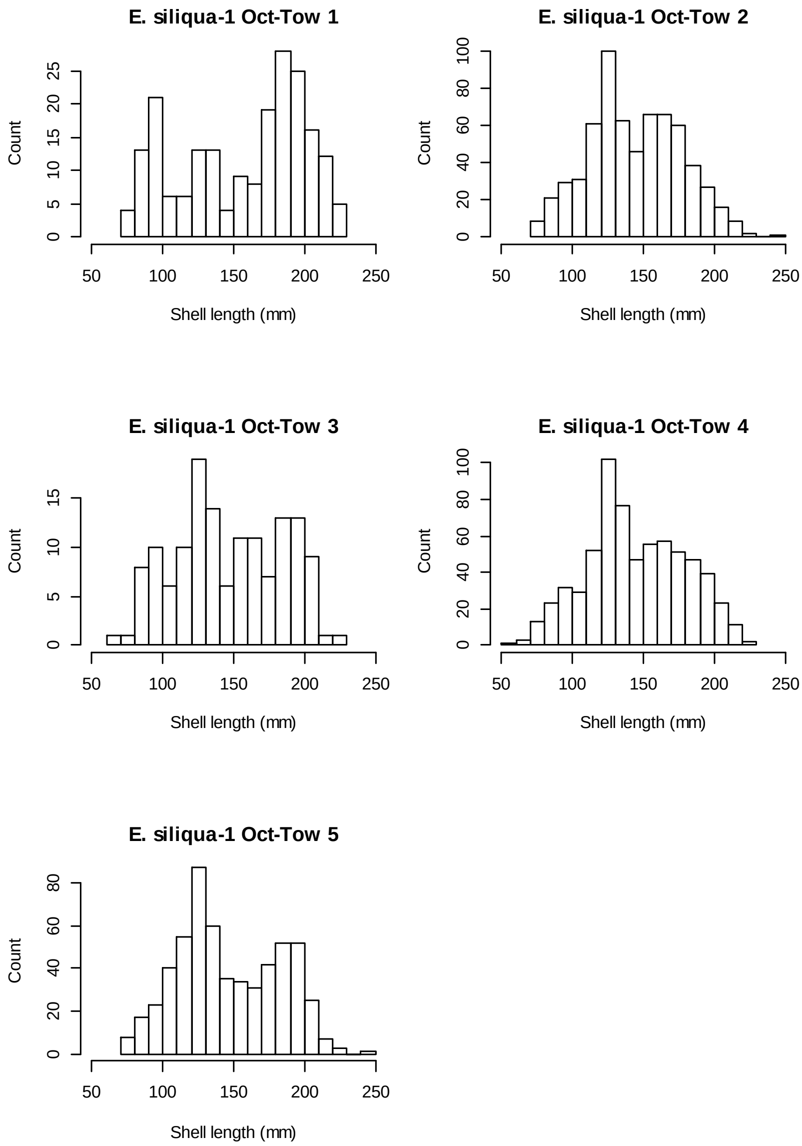

Figure 30: Size frequencies of shell lengths of whole *E. siliqua* measured from towed video collected on 1st Oct, SE of Fuday.

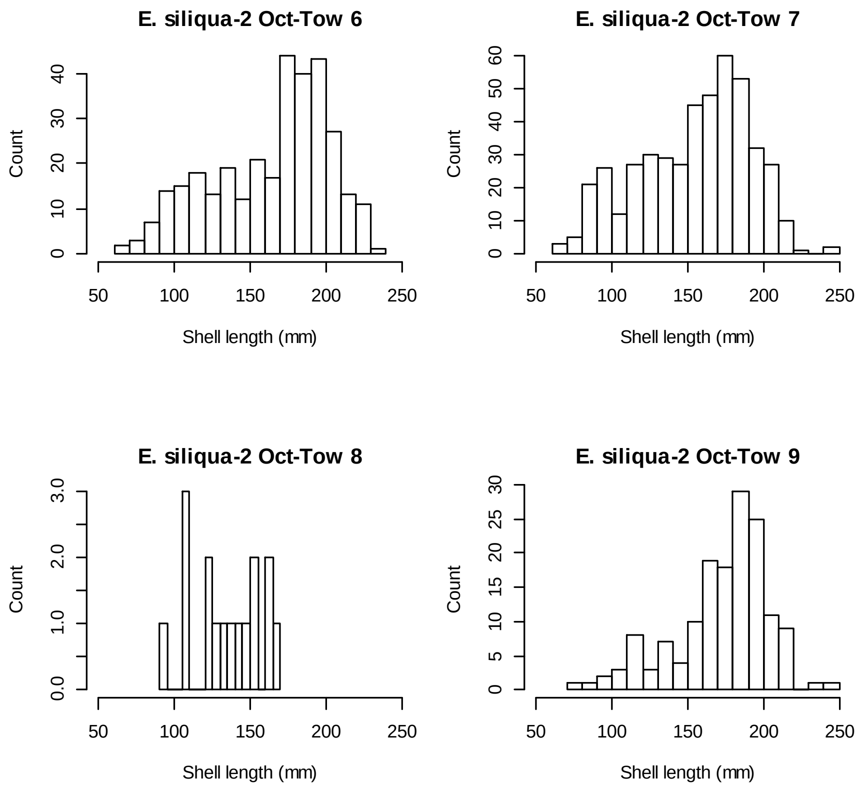

Figure 31: Size frequencies of shell lengths of whole *E. siliqua* measured from towed video collected on 2nd October, Sound of Eriskay.

Smaller numbers of *E. arcuatus* were identified from the videos (Tables 6 and 7). Of the total number of *Ensis* identified on the videos only 6.7% were assigned as *E. arcuatus*. Shell lengths for this species were therefore pooled by sampling site in order to obtain enough measurements (Figure 32). The populations appeared to be comprised of one, or possibly two, size groups with modal lengths at around 120 and 140-150 mm. Separation of groups by length was much less clear than for *E. siliqua*.

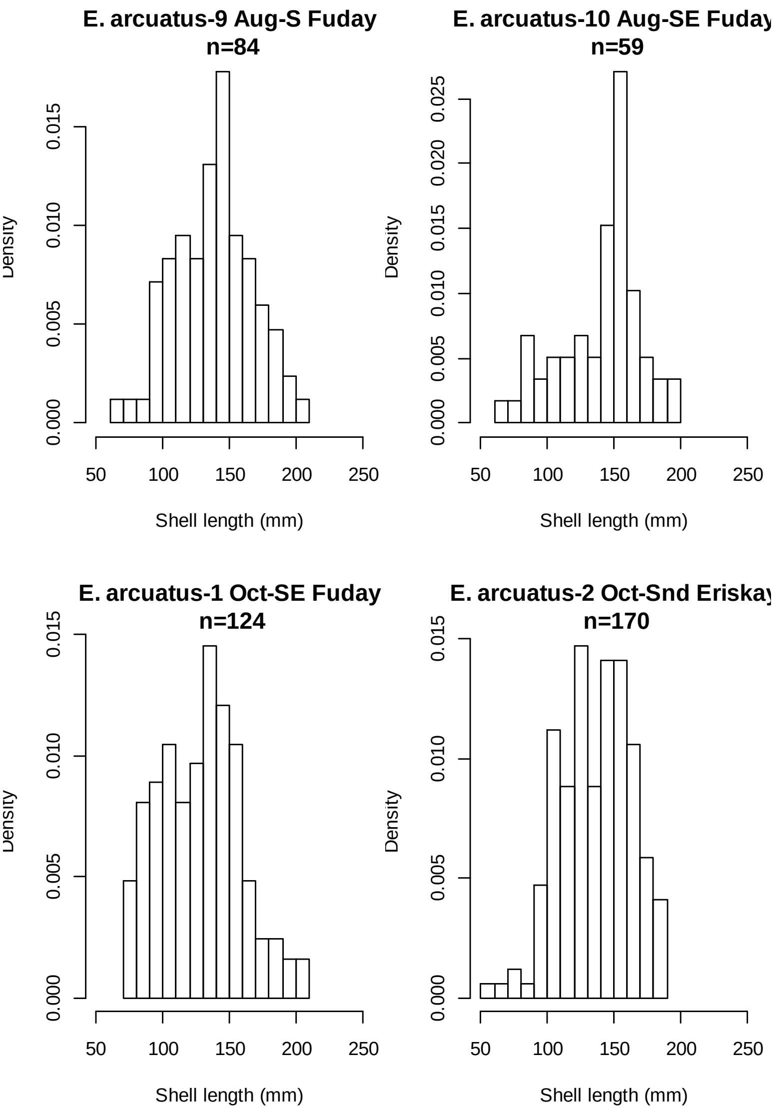

Figure 32: Size frequencies of shell lengths of whole *E. arcuatus* measured from towed video collected on 9th Aug, S of Fuday (top left); 10th Aug, SE of Fuday (top right); 1st Oct, SE of Fuday (bottom left) and 2nd Oct, Sound of Eriskay (bottom right).

The frequency of each length class is shown as a proportion so that the distributions across sites can be compared even though different numbers of clams were measured.

Density Estimates of the Razor Clams

Although the percentage of clams lying partially across video frame edges was low (12% for *E. siliqua* and 5% for *E. arcuatus*) counting each of these as one individual within the swept area would bias the density estimates upwards. It was therefore assumed that, on average, each clam lying across the swath boundaries would contribute 0.5 an individual count. The overall densities of *E. siliqua* thus ranged from 0.15 to 3.02 m^{-2} (Tables 6 and 7). *E. arcuatus* were less common with densities ranging from 0.03 to 0.22 m^{-2}, except for tow 8 in the Sound of Eriskay where the density was 0.93 m^{-2}. As mentioned previously this station was regarded as being anomalous having coarser sediment than the other tows further to the east. Based on the replicate tows undertaken in each area, average densities per site were estimated to be between 1.42 and 2.25 m^{-2} for *E. siliqua* and 0.10 and 0.14 m^{-2}

for *E. arcuatus* (Table 8). The 95% Students-t confidence intervals for the means are clearly large and encompass a zero density in some cases. This low precision is due to the small number of tows generating each mean estimate. Since the main purpose of the project was to examine the feasibility of conducting stock assessments the remainder of the analysis is concerned with a consideration of ways to improve the precision of the mean density estimates.

Table 8: Average densities of razor clams estimated for each fished area ± the normal distribution based 95% confidence interval.

Area	Trip	Number of tows	*E. siliqua* (number m^{-2})		*E. arcuatus* (number m^{-2})	
			Mean	±95% conf	Mean	±95 % conf
S Fuday	1	5	1.42	0.60	0.12	0.05
SE Fuday	1	4	2.25	1.00	0.14	0.07
SE Fuday	2	5	1.97	1.29	0.10	0.08
Sound of Eriskay	2	3[i]	1.53	1.30	0.13	0.21

The most common approach to improving the precision of mean estimates is to increase the number of samples, providing these are independent and ideally randomly spatially distributed within the survey area. The simplest approach to achieving this would be to reduce the length of each tow, so that more tows could be conducted each day of sampling. However, our experience showed that deployment and recovery of the electrofishing gear took around 15 mins for each operation. This fixed time (approximately 30 mins on each tow) needs to be factored in to any consideration of the number of tows of varying lengths which could be achieved per day of surveying.

[i] For the Sound of Eriskay, tow 8 was excluded because the ground was noticeably different from the remaining tows conducted further to the east.

Clustering of ***E. siliqua*** along the Tows

The distributions of individual *E. siliqua* along the tow tracks are shown in Figures 33 to 36 as counts per meter of tow (equivalent to 1.5 m^2 swept area except for Trip 1, tow 9 where the swath width was 1.18 m). The position of any individual clam along the track will however be somewhat imprecise because partially stunned clams were frequently observed moving about using foot kicks. Based on observations on the videos these movements might have shifted the locations of animals from their emergence points by anything up to 1 m.

There are clearly patches where clams were observed more frequently but such clustering can occur even if the animals are randomly distributed in space. Various approaches to testing whether animals are randomly spaced are discussed in Pielou (1977) but all the methods described have restrictions. In general, it can be assumed that organisms, such as clams, are likely to be clustered so simple analyses of precision versus sampling design trade-offs based on simple parametric models, such as the Poisson distribution, may give misleading results. For this reason a boot-strap approach was used for estimating the relationship between precision, length of tows and number of replicate tows for each sampling region based on the observed data.

This part of the analysis was only undertaken for *E. siliqua* which would be the main target of harvesting. Stock assessment for *E. arcuatus* would be even more challenging because of its low densities.

Figure 33: Distribution of counts of *E. siliqua* along the tow tracks from videos collected on Trip 1, S Fuday. Right hand plots show the autocorrelation function, blue dashed lines are the 95% critical levels.

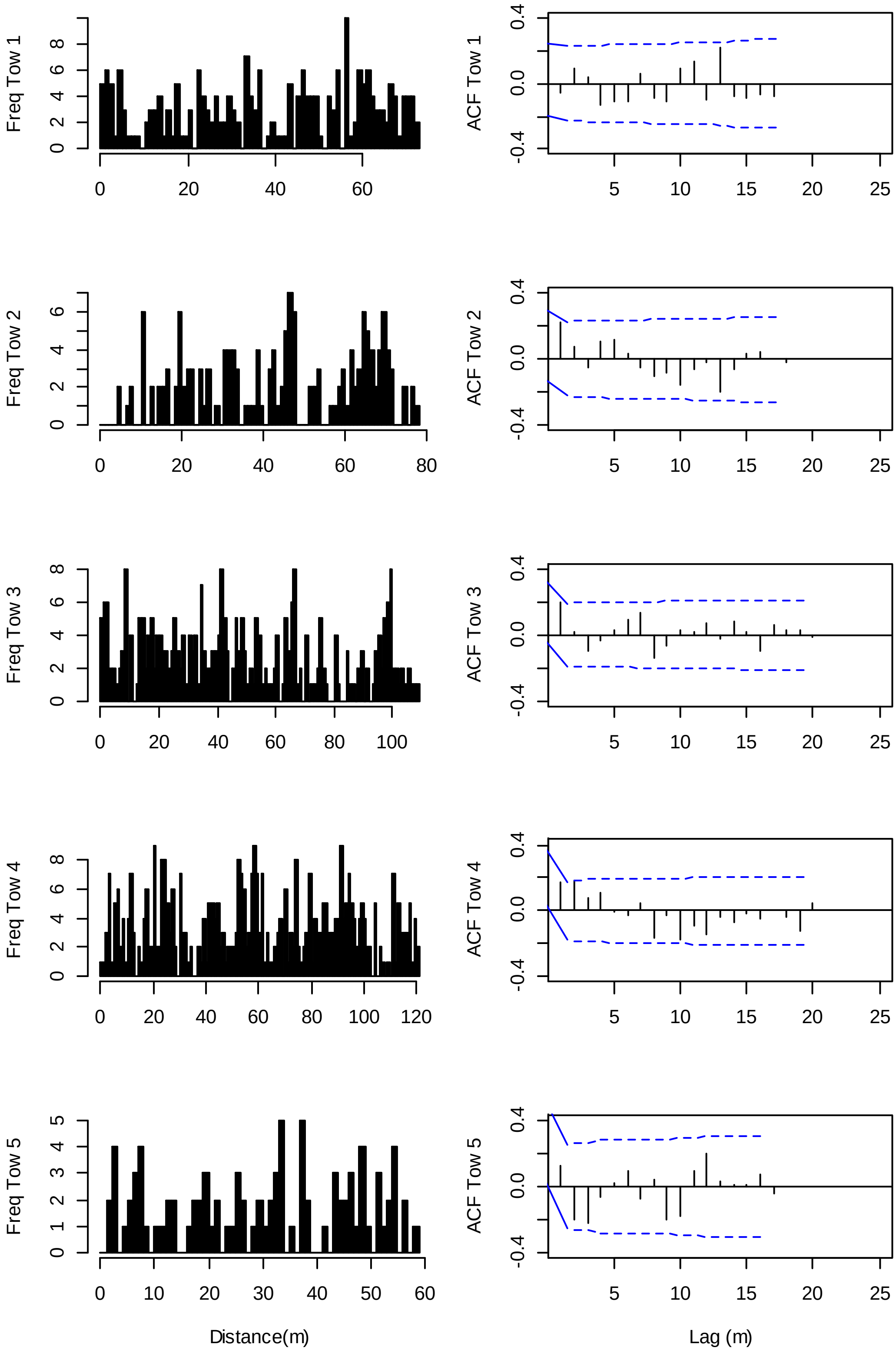

Figure 34: Distribution of counts of *E. siliqua* along the tow tracks from videos collected on Trip 1, SE Fuday. Right hand plots show the autocorrelation function, blue dashed lines are the 95% critical levels.

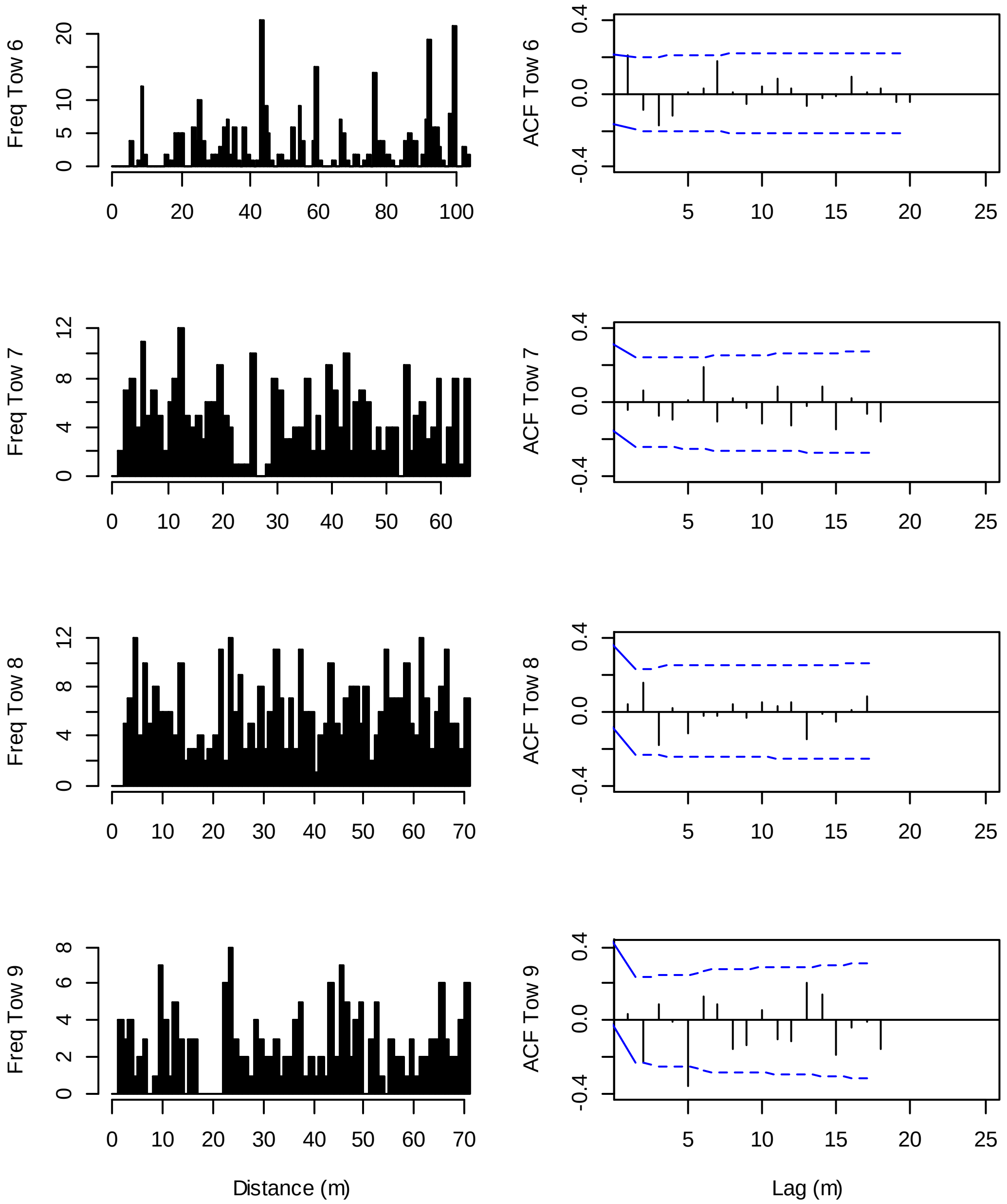

Figure 35: Distribution of counts of *E. siliqua* along the tow tracks from videos collected on Trip 2, SE Fuday. Right hand plots show the autocorrelation function, blue dashed lines are the 95% critical levels.

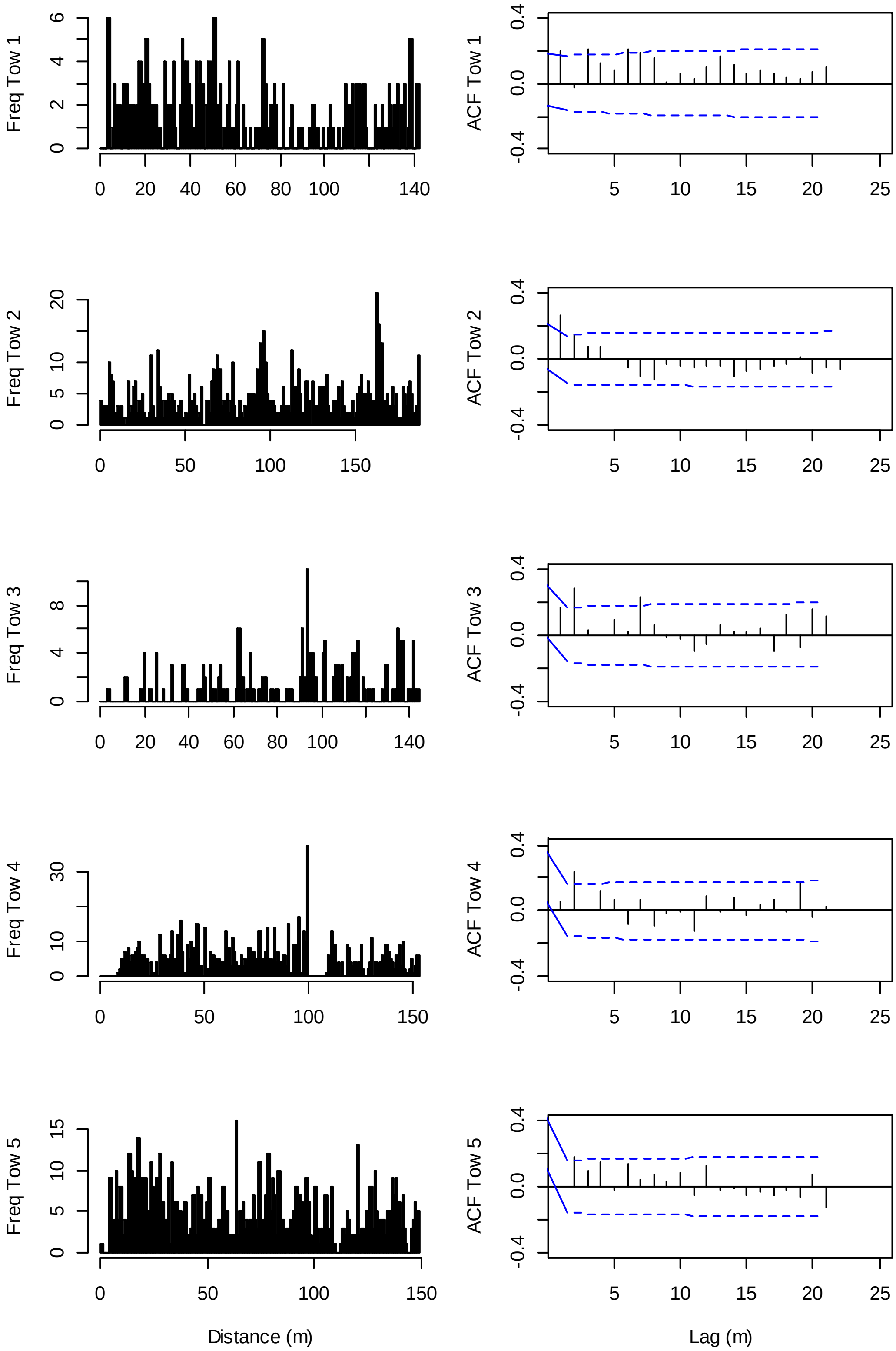

Figure 36: Distribution of counts of *E. siliqua* along the tow tracks from videos collected on Trip 2. Right hand plots show the autocorrelation function, blue dashed lines are the 95% critical levels.

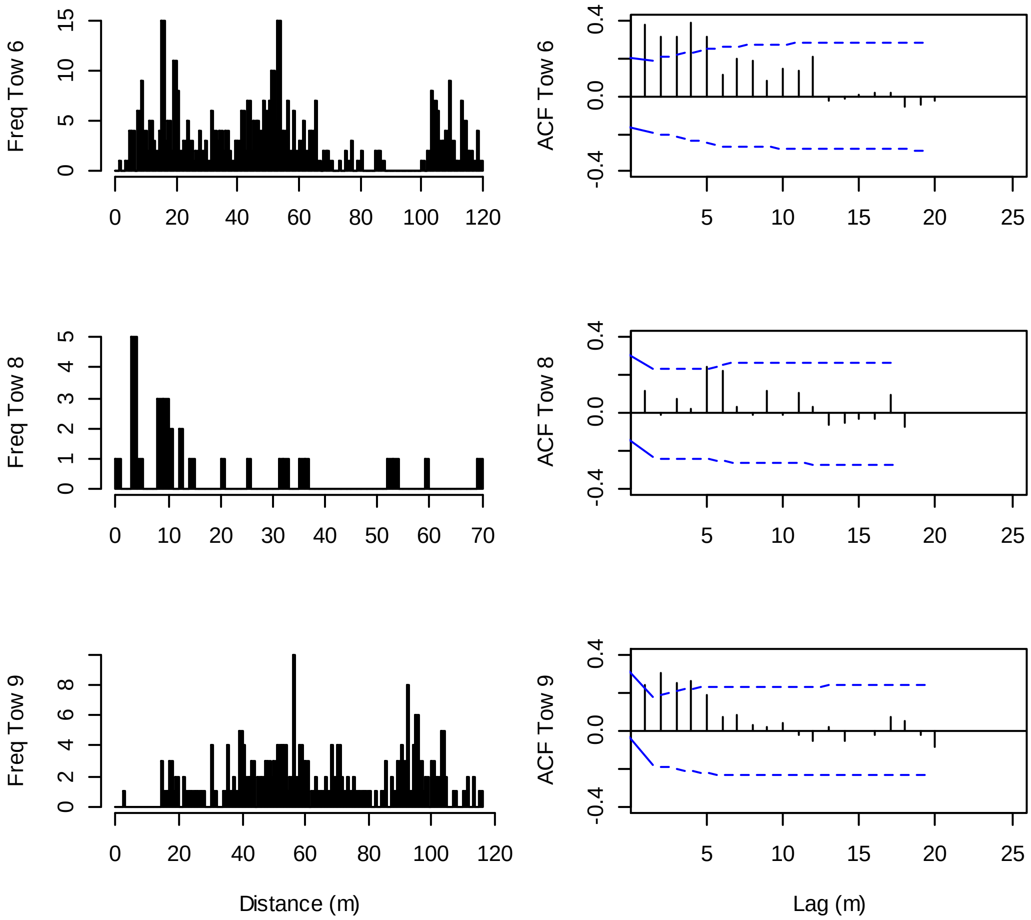

Potential for Increasing the Precision of the Mean Density Estimates by Conducting Shorter Tows

The autocorrelation functions for tows conducted to the S and SE of Fuday (Figures 33 to 35) suggested that there was no significant autocorrelation in counts of *E. siliqua* with distance at separations greater than 2 m, except for one tow (trip 2, tow 3) where there was significant autocorrelation out to 7 m. Tows conducted in the Sound of Eriskay (Figure 36) appeared slightly different with some evidence of significant autocorrelation in counts out to distances of around 5 m. There was no obvious reason for these differences between sites but the occurrence of *E. siliqua* might be influenced by fine-scale differences in sediment which could be aligned spatially by the tidal currents. However, further sampling would be required to fully investigate the spatial distributions of the clams at these scales.

A bootstrap approach was used to further investigate the relation between tow-length, number of replicates and resulting precision. The observed counts of *E. siliqua* were pooled by sampling day and then split into 5 m distance bins producing a total of 90 tow segments for trip 1, day 1 (S Fuday); 50 segments for trip 1, day 2 (SE Fuday) and 157 segments for trip 2 day 1 (SE Fuday). Trip 1, tow 9 (SE Fuday) was excluded from this analysis because of the failure of the middle camera which would affect the total counts. Tows made in the Sound of Eriskay (trip 2, day 2) were also excluded from this part of the analysis because the video failed to vertically stitch for tow 7 and tow 8 was considered anomalous because of the obvious difference in bottom sediment coarseness resulting in a relatively small amount of observational data from this site.

A thousand simulated tows of varying total lengths (10, 20, 30 … 100 m) were then generated by randomly selecting sufficient 5 m tow segments (with replacement) to the required total tow lengths. The total number of clams counted in each simulated tow was then extracted with clams which were lying across video boundaries being assigned a weight of 0.5. The total counts were then converted to density estimates (counts m^{-2}) by dividing by the appropriate swept area (simulated tow length * 1.5 m).

Each pool of 1000 simulated tows was then resampled 200 times (without replacement) to produce sets of random replicates (3, 5, 10, 20…50 repeat tows of each length). The average clam densities in each of the simulated samples were then computed and their 97.5% upper and lower quantiles extracted.

The results (Figure 37) suggest that tow length has little impact on precision once total tow length exceeds about 30 m. In contrast, the number of replicate tows has a stronger influence, but there is little further gain in precision when more than 20 replicate tows are made. The results are of course influenced by the variability in the underlying data so that trip 1, day 1 showed better precision compared with the other sampling days.

Based on the available data it is recommended that an optimal sampling strategy using the combined electrofishing-towed video camera array would be to conduct at least 20 tows of around 30 m length. Taking into account the time required for setting up and retrieving the equipment, each tow would take around 45 mins so that 20 tows of this length would take 15 h of survey time or around 2 days assuming an 8 h working day on site.

This conclusion is based on an assumption that the survey is being conducted across an area of reasonably homogenous sediment and that the variability and density in clam counts will be similar to that seen within the sites sampled in this project. Variations in factors such as sediment or depth across a complete razor clam bed might require further stratification of the sampling area thus increasing survey effort.

Figure 37: Results of estimating precision as upper and lower 97.5% quantiles from simulated mean density calculations based on varying total tow length and the number of replicate tows.

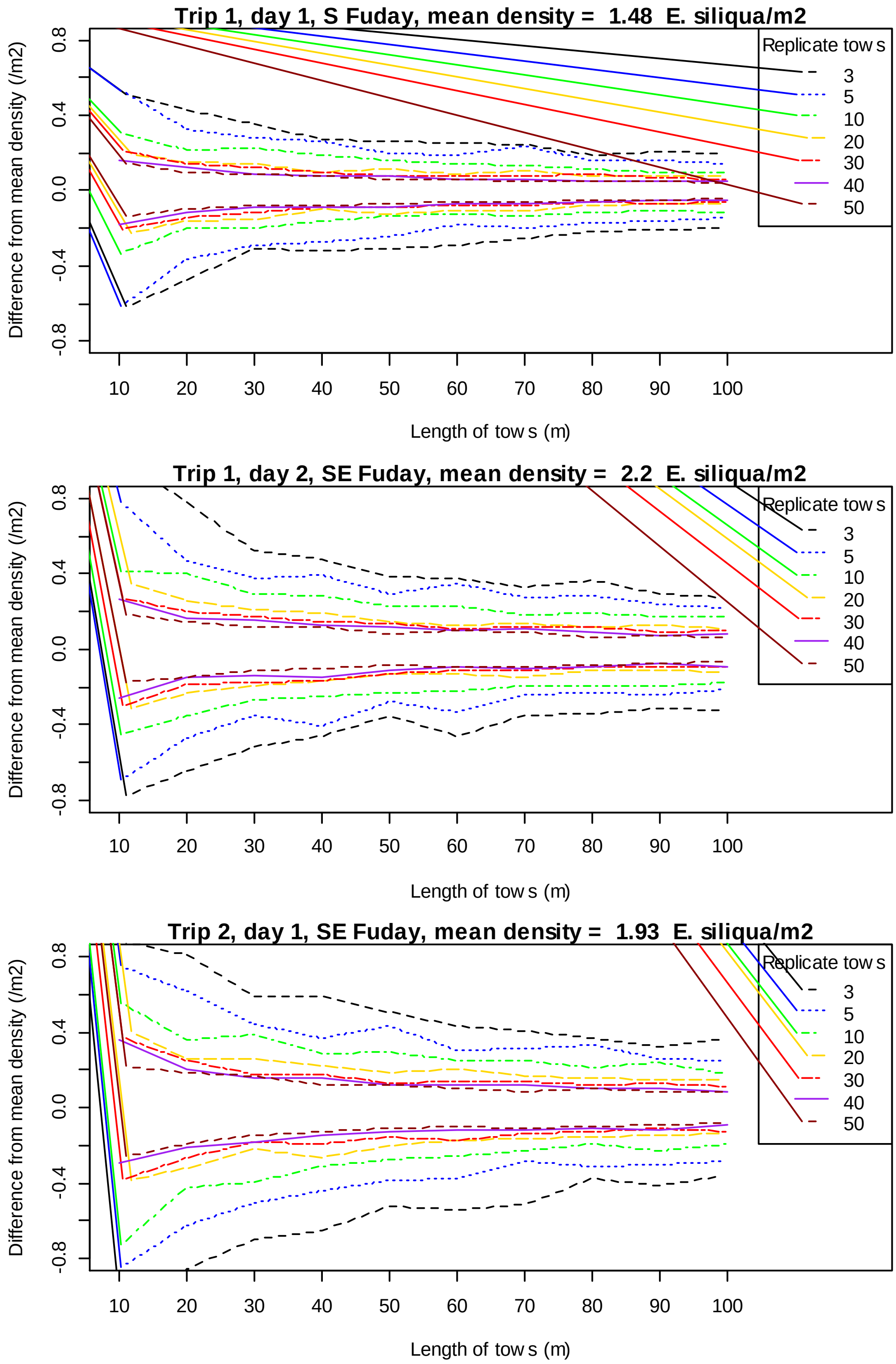

Potential for a Drop-down Electrofishing Camera System to Increase Precision

As mentioned previously the time required to deploy and recover the towed electrofishing-video rig was substantial and becomes an increasing fraction of total tow duration as tow lengths are reduced. An alternative to the towed equipment could be a dedicated drop-down camera (Figure 38) which should be quicker to deploy and recover, would not require a diver and could also overcome the issue of emergent clams moving out of the sampling quadrat. However, this device has not yet been constructed or tested so the following considerations remain theoretical. Some practical problems can also be foreseen since the deploying vessel will be moved by the tide and wind during sampling during which the device would need to be stationary on the seabed. Exposure times of between 30 seconds to two minutes are required to ensure all clams emerge (Murray et al. 2014). Typical peak tidal flows around the western Isles are up to 2 knots which would carry the sampling vessel around 120 m from the sampling location in this time. The deployment of a drop-down camera system would therefore probably be limited by tidal state. Alternatively it might be possible to deploy such a drop-down camera using fly-dragging i.e. using a fixed anchor to limit the vessel movement in a manner similar to the operation of the towed rig (Figure 1) but this latter approach brings in some of the problems seen with the towed-rig in terms of applying a spatially random sampling design.

If these practical problems could be overcome such a device should be quicker and easier to deploy from a range of survey vessels, would not require the use of divers for setting and recovering the gear and would restrain emergent clams from moving out of the video field of view (and prevent clams moving in from outside). Sampling at point locations also has some statistical attractions in that a properly randomised spatial design can be used.

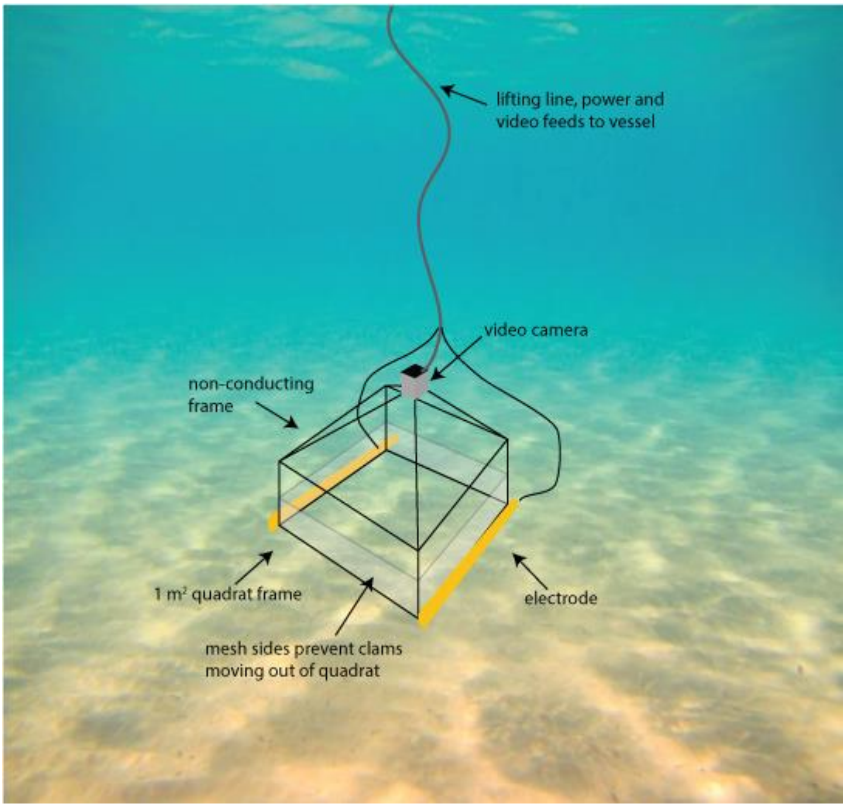

Figure 38: A potential design for a combined electrofishing drop-down camera.

However, to be practical in operational terms such a drop-down device would probably only image around 1 m2 of seabed, resulting in a large fraction of the observed quadrats having zero counts (Figure 39).

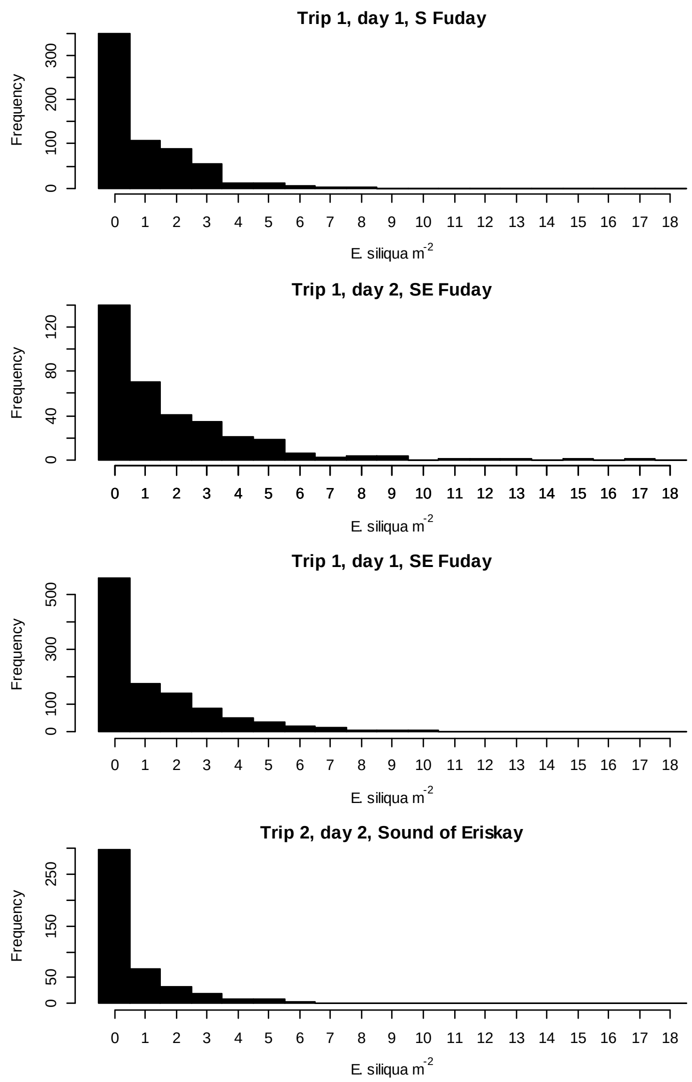

Figure 39: Distributions of observed counts of *E. siliqua* in the total video collected at each site when the video was split into fragments equivalent to 1 m^2 of seabed.

On trip 1, day 1 there was a single observation of a density of 36 m^{-2} which is not shown.

Fitting Poisson distributions to the data confirms that there are more zeroes than would be expected under the model assumption that the clams are distributed randomly within the 1 m^2 areas. Such patterns are common with biological data but will impact the relationship between sample replication and precision of mean density estimates.

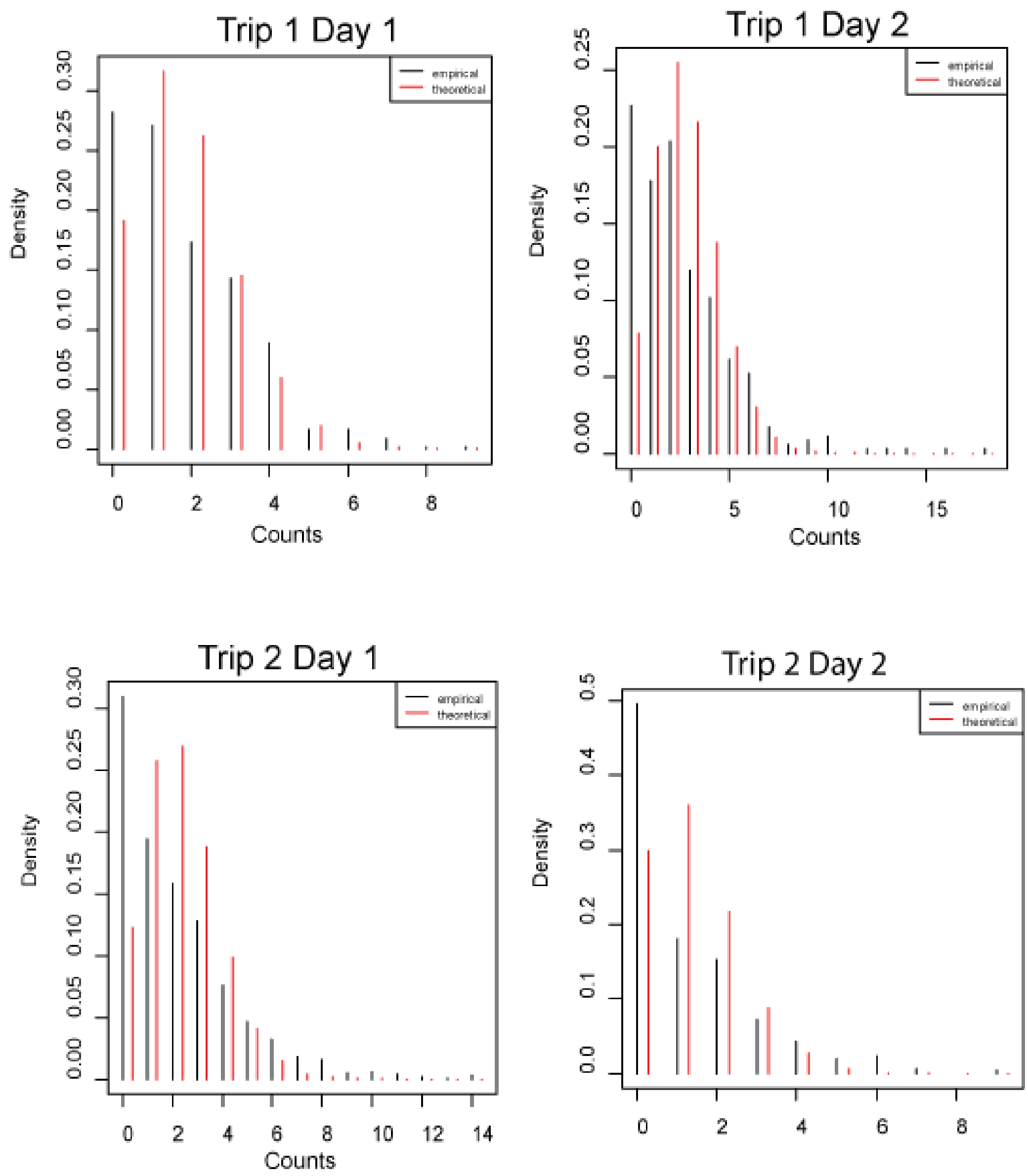

Figure 40: Poisson distribution fits to the counts of *E. siliqua* in the total video collected on each day.

The likely relationship between replication and precision based on 1 m^2 sampling was therefore assessed using a similar boot-strap procedure as described above but re-sampling the original video data in 0.7 m distance bins (area = $1m^2$). The predicted relationship between precision and number of drop-down deployments for each survey region is shown in Figure 39. Compared with the towed camera results (Figure 37) a much larger number of deployments is required before the improvement in precision stabilises. This value appears to be around 300 replicate drops, but even at this level of sampling the achieved precision is poorer than with the towed camera.

Further exploration of the likely precision using larger imaged areas might be worth exploring although an electrofishing-camera system imaging a larger area of seabed might be impractical to deploy.

Figure 41: Results of estimating precision as upper and lower 97.5% quantiles from simulated mean density calculations based on varying the number of drops made using a theoretical combined electrofishing drop-down camera imaging $1m^2$ of seabed.

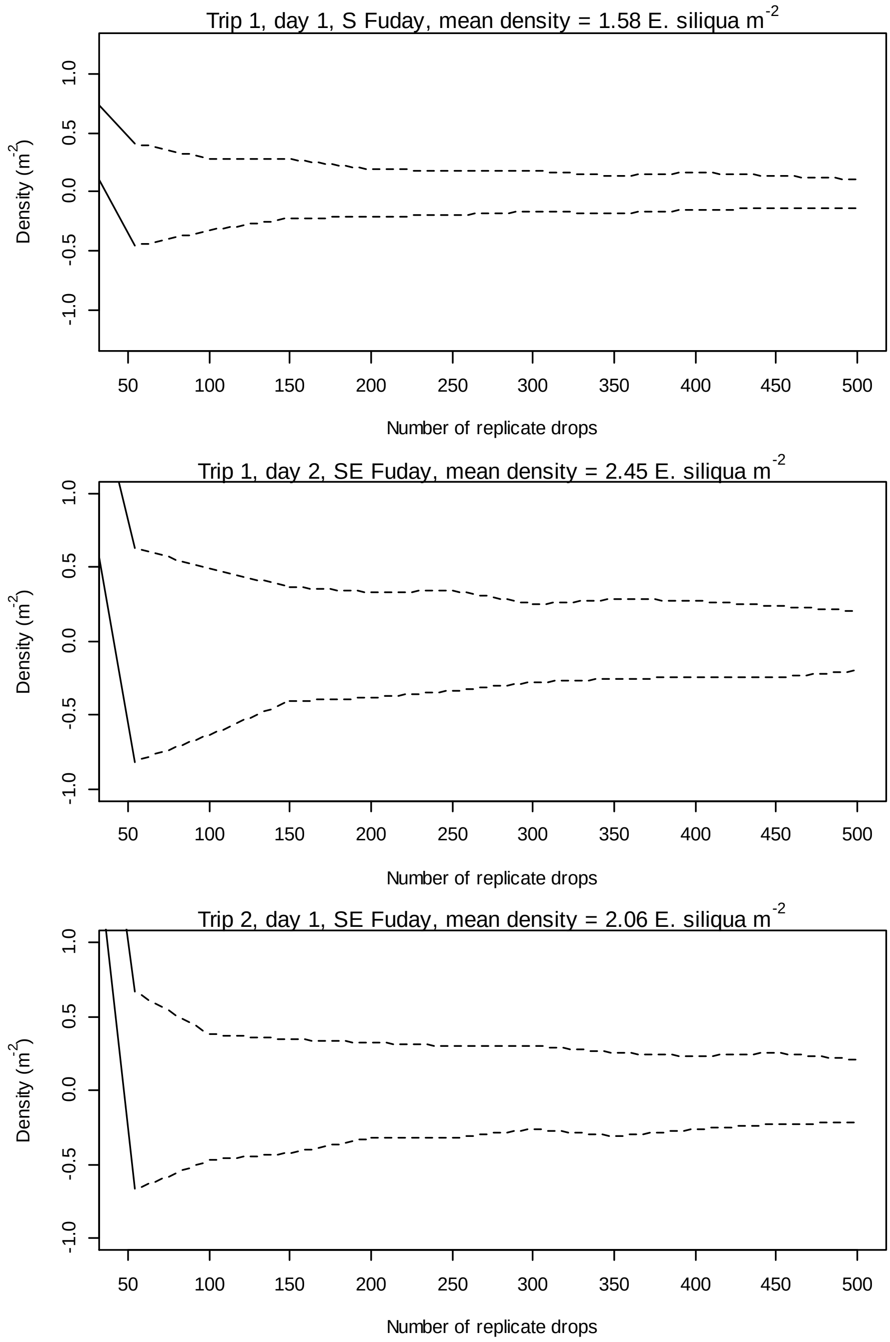

Costs for Conducting Surveys Using the Electrofishing-Video Technique

An indication of the resources needed for surveying using the towed electrofishing-video approach is given in Table 9. The final cost for producing a stock assessment on a particular bed would require more detailed analysis taking into account the extent of the bed, the number of tows required to achieve the desired precision, the distance of the bed from the survey vessel home port and the cost of survey and data analysis staff.

Table 9: Indicative costs of conducting a razor clam stock assessment by combined electrofishing-towed video.

Item	Quantity	Cost	Notes
Electro-fishing rig and ancillary equipment	1	£6000	Woolmer et al. (2011) but includes costs of diving gear etc. which vessel operator may already have
Towed camera rig	1	£2000	
Vessel hire (per day)	1	£2-4,000	Depending on vessel type
Travel time to survey area (depends on location)	Variable	Staff time	This project
Minimum number of 30 m (15 min) tows	20	Staff time	This project
Days surveying (assumes 5-10 tows d^{-1} depending on conditions)	2-4 days	Staff time	This project
Matlab commercial licence with image processing toolbox	1	£2,700 +VAT	MathWorks
Post-processing video		Overnight per hour of video collected	Runs automatically
Identification and measurement of clams on the video	5 hours	On average an hour of staff time per hour of video collected	This project
Analysis of data and report writing	1-2 days	Staff time depends on scale of survey conducted	

Discussion

General Discussion

Commercial electrofishing gear appears to be highly efficient at forcing razor clams to the surface and the technique thus has the potential to lead to rapid depletion of razor clam beds. Given this risk, both Breen et al. (2011) and Murray et al. (2014) emphasised the need to develop robust stock assessments for razor clams before any potential legalisation of this technique. As described in the introduction to the present report most previous attempts at razor clam stock assessment have used commercial dredges or divers. However, dredging is acknowledged to cause habitat damage as well as leading to ancillary damage to the clams themselves. Furthermore, dredges do not usually catch all sizes of clams and so will only produce a partial assessment of the population (Fahy & Gaffney 2001). Salting or hand-pulling, while causing relatively little habitat damage, is expensive and appears to be a rather inefficient approach to conducting stock assessments in sub-tidal areas (Fahy et al. 2001).

Based on the results of the present study, combining electrofishing with a towed video camera array appears to offer several advantages over these alternate survey techniques. Electrofishing seems to cause relatively little habitat impact (Breen et al. 2011, Murray et al. 2014), appears to be efficient in forcing clams of all sizes to the surface (Murray et al. 2014), and recovery rates of the clams after the rig has passed over are thought to be high (Murray et al. 2014). In the present study a number of both stupefied and mobile non-target organisms were observed with shore crabs (*C. maenas*) being most common. Murray et al. (2014) tested the effect of simulated electrofishing on a variety of non-target organisms including starfish (*Asterias rubens*), hermit crabs (*Pagurus bernhadus*) and surf clams (*Spisula solida*). Starfish appeared to be unaffected, hermit crabs retreated into their shells and surf clams either exhibited a kick-response or failed to react. For fish, Murray et al. (2014) reported that they were able to collect stunned sandeels (*Ammodytes marinus*) whilst electrofishing at sea and that these animals recovered within 10 minutes of being removed from the electrical field. Stunned organisms may however be vulnerable to predation whilst recovering on the seabed. Video observations by Albalat et al. (2016) suggested that predators (shore crabs and squat lobsters *Munida rugosa*) were attracted to small discarded *Nephrops norvegicus* recovering on the seabed after being caught in trawls in as little as ten minutes. Attraction of predators to areas disturbed by large commercial beam trawls has also been recorded by Kaiser et al. (1994) and Ramsay et al. (1996). However, the electrofishing rig does not mechanically damage non-target organisms which should reduce the scent-plumes released from injured animals. Predation rates during organism recovery may thus be lower for electrofishing when compared with commercial beam trawls.

As mentioned in the introduction there is little historical data with which to compare our results. Based on reported catches in commercial dredges, Fahy and Gaffney (2001) estimated the mean density of *E. siliqua* at Gormanstown, Ireland to be 1.45 animals m^{-2}. Murray et al. (2014) reported some local density estimates for *Ensis* (both species combined) made by divers while conducting experimental electrofishing in the west of Scotland at up to 17 clams m^{-2}. Splitting the video collected in the present study into 1 m^2 segments suggested that local densities of *E. siliqua* ranged between 0 and 18 m^{-2} (with a single observation of 36 m^{-2}). The average densities for *E. siliqua* estimated in the present study (1.42-2.25 m^{-2}) thus appear quite reasonable when compared with the limited observations reported from elsewhere.

In terms of individual sizes the populations of *E. siliqua* sampled in the present project were generally dominated by larger specimens. Most of the observed size frequencies were polymodal, a feature also seen in razor clam samples from Ireland (Fahy & Gaffney 2001). The samples in the Irish study were collected using commercial dredges and the authors noted that smaller clams would not be retained by that gear. Since the response of razor clams to electrical stimulation is not supposed to be affected by their size (Murray et al. 2014), we were expecting to see a higher proportion of smaller animals in our video-survey results. However, McKay et al. (1992) also commented that established razor clam beds around Scotland tended to be dominated by larger individuals.

A similar pattern was found with regard to the sizes of *E. arcuatus* with the sampled populations being mostly dominated by larger individuals. Fahy et al. (2001) showed that smaller *E. arcuatus* tend to occur outside of the main beds and may only recruit as larger individuals are removed or die.

In conclusion, little appears to be known regarding the recruitment dynamics of razor clams. Because of the mobility of clams it has been stated that harvested areas can be re-colonised, but only if there are sufficient clams in surrounding areas (Fahy et al. 2001). It has also been observed that intense harvesting can lead to changes in the overall community structure resulting in very slow rebuilding of the *Ensis* populations (Fahy and Carroll, 2007).

Precision of Mean Density Estimates

The main questions regarding the use of electrofishing-video as a stock assessment tool relate to the precision of the resulting density estimates and the costs of conducting such surveys. The distribution of razor clams is patchy and sampling such animals is widely acknowledged as being statistically challenging (Miller & Ambrose 2000). In the present study, the analysis of razor clam patchiness along the tows showed significant autocorrelation in counts only at small distances (<5 m) suggesting that clam abundance is not structured with any regular pattern. Providing sampling units are kept at around this level the resulting samples should be reasonably independent.

Increasing sample replication will normally improve precision of mean estimates and in this case implies a need to perform shorter tows. However, our experience on the present project showed that the deployment and recovery of the electrofishing rig is quite time consuming and this needs to be factored in to these considerations. Re-sampling of the video data suggested that precision around the mean densities does indeed improve with increasing tow length, but that this improvement tends to stabilise when tows are about 30 m in length. Precision of the mean density estimates was more strongly affected by the number of tows although there did not seem to be much further improvement beyond 20 replicates. It must also be remembered that these predictions are based on re-sampling the data collected in the present study and would be affected by any differences in clam densities and distribution patterns at other sites. It might also be necessary to adopt stratified survey designs for beds with greater variability in sediment type or depth and this would increase the amount of replication required.

Drop-down Versus Towed Approaches

An alternative to using a towed electrofishing-camera combination could be to design a drop-down system which would stimulate a small area, perhaps 1 m^2, of seabed with observations of emergent clams being recorded by video. This would be similar to the design used by Murray et al. (2014) for monitoring the recovery of benthic organisms after experimental electrofishing. This approach would essentially be quadrat-based, which is a widely used technique for estimating benthic populations in inter-tidal areas and where the statistical properties of such sampling are well understood. We did not test this approach in the field because the original project proposal envisaged this as a back-up option if the towed camera rig proved impractical. Based on our experience in the present project we envisage at least two problems with operating such a drop-down electrofishing-camera. Firstly, the tidal currents in the areas fished (excepting the Sound of Eriskay where the causeway restricts the tidal flow) were relatively strong. Because the electrofishing field generally needs to be applied to an area of seabed for between 0.5 to 2 minutes to stimulate the emergence of all the razor clams (Murray et al. 2014), the deploying vessel would be moved some distance from the deployment location in this time. This could probably drag the drop-down electrofishing-camera rig along the seabed. A potential solution could be to use a fixed anchor to prevent vessel drift in a similar manner to fly-dragging the towed electrofishing rig. If the problem of drift could be overcome the deployment and recovery of such a drop-down electrofishing-camera should be much faster than for the towed rig used in the present study. However, the clustered distribution of clams will also result in zero counts in a large number of the relatively small, 1 m^2 quadrat-frames. The towed camera approach addresses this issue by sampling a much larger area, albeit with a trade-off against a purely randomised survey design and the time needed for deployment and recovery of the equipment. We conclude that the towed approach is probably preferable, as supported by the re-sampling simulations of the relationship between replication and precision, although further investigations of larger quadrat designs could be made (Figures 37 and 41).

Issues with Towed Approach

We assumed that all razor clams present would be forced to the surface by the electrofishing rig. The assumption of high efficiency seems reasonable based on experimental work by Murray et al. (2014) where electric fields stimulated 100% of test animals to emerge. The efficiency with which razor clams are stimulated to emerge will also be affected by the speed at which the electrofishing rig is towed over the seabed, in particular if the rig moves too rapidly that patch of seabed may not be stimulated for long enough. In the work conducted by Murray et al. (2014) tow speeds varied from as little as 1 m min^{-1} to as high as 10 m min^{-1} (average 3 m min^{-1}). The corresponding maximum and minimum exposure times of organisms to the electric field were estimated to be between 3 and 0.33 minutes. Average speeds over the ground in the present study varied between 1.2 and 3.2 m min^{-1} which are towards the lower values given by Murray et al. (2014). We therefore expect that the periods of exposure to the electric field were sufficient in the present study. However, there were times when, due to varying tidal and wind conditions, the speed of the electrofishing-camera rig over the ground became excessive. The live video feed was extremely valuable in these situations as it allowed prompt corrective action taken.

Although most of the clams were stationary on the videos mobile individuals were also observed. Such movements could take individual clams out of the video field-of-view before the camera rig arrived above them. Because the electrofishing rig was about twice as wide as the video swath it seems reasonable to assume that similar numbers of clams might, on average, move into the video-frame from the electrified areas lying to either side. The directions of movement of clams behind the electrofishing gear probably requires some further research to establish that individual movements are not causing a bias in the counts beneath a centrally located towed video camera array.

The towed camera technique was clearly impacted at some sites by the presence of dense seagrass or macro-algae. Although the majority of the video obtained to the south and southeast of Fuday was clear, obstruction with weed was a particular issue in the Sound of Eriskay. Video observations in such areas are likely to underestimate the true population because not all the clams present will be visible. This problem will apply to any camera-based survey technique and probably only the use of divers could overcome this problem.

Video Camera Performance

We did experience one camera failure on trip 1. This appears to have been caused by movement of the power/signal cable where it enters the rear of the camera housing leading to a failure of the waterproof seal at this point. Following this incident all these connections were strengthened by embedding the rear of the cameras plus a short length of the connection cable in resin (Polycraft FC-6600 slow-setting polyurethane, MB Fibreglass, Newtonabbey, UK). No further camera failures occurred.

The Sony cameras used are relatively cheap (around £180 each) and are only rated down to 50 m but this was perfectly adequate for this application. Being able to monitor the video in real-time aboard the vessel proved extremely useful in comparison to being only able to evaluate footage after a tow was completed (for example if we had used GoPro cameras). The low light performance of the Sony cameras was particularly good and no problems were experienced with illumination. Some slight differences between the cameras were noted in terms of the correction factors which had to be applied for picture distortion and some distortion was still apparent at the edges of the images after processing. These differences are probably the result of slight variations in the camera lenses, or in the orientation of the imaging chip relative to the lens. If the electrofishing-video technique were to be adopted more widely further testing and development using different cameras might be advisable. For example, use of cameras with wider fields of view might reduce the amount of post-processing required to generate a wide swath whilst more expensive cameras/lenses might have more consistent lens distortions. The positive aspects of using the Sony cameras are that they produced satisfactory results and kept the costs of the camera rig at less than £2000.

On one of the tows one of the cameras was knocked slightly out of alignment. The brackets constructed to mount the cameras allowed both the tilt angle and the camera position to be adjusted horizontally. Whilst this was useful in initially setting up and calibrating the camera rig, totally rigid brackets would be preferable for longer term operation.

Costs of Conducting a Stock Assessment using a Towed Electrofishing-Video Camera Rig

Given the low cost of constructing the equipment, the main costs for conducting stock assessments using the electrofishing-video method relate to vessel hire and to the staff time required for collecting and analysing the data. Our experience in the present project suggests that one needs to allow around 30 mins per tow to recover the equipment, move to the next location, reset the vessel anchor and redeploy the gear. Realistically this means that between five and ten, 30 m tows could be undertaken per day, depending on conditions.

The main issue in determining survey costs will then be the number of tows required to estimate the razor clam populations with an acceptable precision. Our re-sampling simulation suggested that precision would stabilise at around 20 replicate tows. Such a survey might therefore be completed in 2 to 4 days depending on how many tows can be completed each day. Survey costs could be reduced by making fewer tows if one is prepared to accept the resulting loss in precision.

Although the post-processing of the video proved extremely time-consuming (1 h of video took around 4 h to horizontally merge and 3-5 h to vertically stitch), the Matlab programs written for this project (Appendices 1 and 2) meant that these steps could be left to run unattended overnight. The interactive collection of razor clam length measurements using the Matlab program written for the project (Appendix 3) took between 45-60 mins per hour of collected video.

Further Work Required to Develop the Method for Stock Assessment

We suggest a few areas where further development work may be required if the method were to be used for conducting stock assessment surveys of razor clams.

1. Further field-based calibration tests are recommended to confirm the accuracy and precision of length measurements reconstructed from the video. In particular, the potential for errors to be introduced due to undulations in the seabed over which the rig is being towed should be addressed. A suitable approach could be to run the camera system over a large number of known length objects (such as the plastic calibration blocks used in the test tank) which would be placed on the seabed (and recovered after the test) to compare the reconstructed lengths with the known lengths.

2. The accuracy of the tow length estimation technique needs further corroboration. Short baseline acoustic positioning could be used to correct the ship GPS positions to the camera locations allowing accurate comparison with the vertical stitching algorithm results.

3. If the combined electrofishing-video method were to be applied more widely for stock assessment it is recommended that a wider range of video cameras be tested. In particular, the field-of-view and the consistency of the lens and chip-induced image distortion should be evaluated between different cameras, makes and models.

4. Synchronisation between the cameras appeared to be out by up to a few frames. This aspect could probably be improved which would help with horizontal montaging of the video streams. The costs of addressing (3) and (4) could however increase the equipment costs substantially.

5. Further consideration of using a drop-down version of the electrofishing-video rig could be worthwhile. This approach could improve the speed of deployment and recovery and remove the need for divers, as well as improving survey design. However, practical difficulties including vessel drift during the time needed to expose the seabed to the electrical field might prove challenging. Drop-down sampling is also likely to generate large numbers of images with zero-counts unless the imaged area could be increased above 1 m^2. The relationship between precision and imaged area thus needs further exploration. The trade-offs between increased statistical rigour versus time and cost would need to be carefully considered when choosing between the towed or drop-down approaches.

Acknowledgements

The author would like to acknowledge the enthusiasm of Duncan MacInnes, Outer Hebrides Inshore Fisheries Group in developing this project, to the skipper and crew of the fishing vessel ‘Lizanna’ (Morrison Shellfish Ltd.) for all their help and local knowledge without which conducting the sea trials would have been impossible; to Lars Brunner (SAMS) for assistance with fieldwork and recording length data from the videos and to Tom Wilding (SAMS) for discussions about the statistical treatment of the data. I also wish to thank Heather Tibbetts (Marine Scotland, Access to Sea Fisheries Team) for her assistance in processing the derogations and to colleagues at Marine Scotland Science, Aberdeen for their helpful advice and comments on this report.

References

Albalat A, Collard A, Bruce M, Coates CJ, Fox CJ (2016) Physiological condition, short-term survival, and predator avoidance behavior of discarded Norway lobsters (*Nephrops norvegicus*). J Shellfish Res 35:1053-1065.

Breen M, Howell TRW, Copland P (2011) A report on electrical fishing for razor clams (*Ensis* sp.) and its likely effects on the marine environment. Marine Scotland Science Report, 120 pp.

Constantino R, Gaspar MB, Pereira F, Carvalho S, Cúrdia J, Matias D, Monteiro CC (2009) Environmental impact of razor clam harvesting using salt in Ria Formosa lagoon (Southern Portugal) and subsequent recovery of associated benthic communities. Aquat Conserv: Mar Freshwat Ecosyst 19:542-553.

Fahy E, Carroll J (2007) Consequences of hydraulic dredging for a razor clam *Ensis siliqua* (L.) bed in the north-west Irish Sea. Biology and Environment: Proceedings of the Royal Irish Academy 107B:115-128.

Fahy E, Gaffney J (2001) Growth statistics of an exploited razor clam (Ensis siliqua) bed at Gormanstown, Co Meath, Ireland. Hydrobiolgia 465:139-151.

Fahy E, Norman M, Browne R, Roantree V, Pfeiffer N, Stokes D, Carroll J, Hannaffy O (2001) Distribution, population structure, growth and reproduction of the razor clam *Ensis arcuatus* (Jeffreys) (Solenaceae) in coastal waters of western Ireland. Irish Fisheries Investigations 10.

Gaspar MB, Castro M, Monteiro CC (1998) Influence of tow duration and tooth length on the number of damaged razor clams *Ensis siliqua*. Mar Ecol Prog Ser 169:303-305.

Gaspar MB, Monteiro CC (1998) Reproductive cycles of the razor clam *Ensis siliqua* and the clam *Venus striatula* off Vilamoura, Southern Portugal. J Mar Biol Assoc UK 78:1247-1258.

Hauton C, Howell TRW, Atkinson RJA, Moore PG (2007) Measures of hydraulic dredge efficiency and razor clam production, two aspects governing sustainability within the Scottish commercial fishery. J Mar Biol Assoc UK 87:869-877.

Henderson SM, Richardson CA (1994) A comparison of the age, growth rate and burrowing behaviour of the razor clams, Ensis siliqua and E. ensis. J Mar Biol Assoc UK 74:939-954.

Holme NA (1951) The identification of British species of the genus *Ensis* Schumacher (Lamellibranchiata). J Mar Biol Assoc UK 29:639-647.

Holme NA (1954) The ecology of British species of Ensis. J Mar Biol Assoc UK 33:145-172.

Kaiser MJ, Spencer BE (1994) Fish scavenging behaviour in recently trawled areas. Mar Ecol Prog Ser 112:41-49.

Marine Laboratory (1998) A study of the effects of water jet dredging for razor clams and a stock survey of the target species in some Western Isles populations. Marine Laboratory, Aberdeen Report, Marine Laboratory, Aberdeen Report, 75 pp.

Marine Scotland (2016) Scottish sea fisheries statistics 2015. Edinburgh, 112 pp.

McKay DW (1992) Report on a survey around Scotland of potentially exploitable burrowing bivalve molluscs. Fisheries Research Services Report, 70 pp.

Miller AW, Ambrose RF (2000) Sampling patchy distributions: comparison of sampling designs in rocky intertidal habitats. Mar Ecol Prog Ser 196:1-14.

Murray F, Copland P, Boulcott P, Rovertson M, Bailey N (2014) Electrofishing for razor clams (*Ensis siliqua* and *E. arquatus*): Effects on survival and recovery of target and non-target species. Scottish Marine and Freshwater Science 14, Marine Scotland Science, Aberdeen, 50 pp.

Pielou EC (1977) Mathematical ecology. John Wiley & Sons, New York, 385 pp.

Ramsay K, Kaiser MJ, Hughes RN (1996) Changes in hermit crab feeding patterns in response to trawling disturbance. Mar Ecol Prog Ser 144:63-72.

Woolmer A, Maxwell E, Lart W (2011) Effects of electrofishing for *Ensis spp.* on benthic macrofauna, epifauna and fish species. SEAFISH Reports, 49 pp.

Appendix 1

Matlab code to allow correction for lens distortion and horizontal montaging of three video camera steams. The output is an .mp4 file from which measurements can be made using the MeasureObjectsFromVideo program (Appendix 3).

Jaap's lens distortion program needs to be installed before running this code and is available at http://uk.mathworks.com/matlabcentral/fileexchange/37980-barrel-and-pincushion-lens-distortion-correction

```
%%%%%%%%%%%%%%%%%%%%%%%%%%%%%%%%%%%%%%%%%%%%%%%%%%%%%%%%%%%%%%%%%%%%%%%%%%%%%%
% C Fox Nov 2016                                                             %
% NOTE This is all based on the Sony 37CSHR cameras which outputs 576x944 %
% % RGB images - if using different cameras which have a different           %
% frame size then the program will need to be adjusted.                     %
%                                                                            %
% Program to take three Sony 37CSHR video feeds as used on the razor         %
% clam sled, correct them for camera distortion so the images are            %
% calibrated to real world distances and combine them into a single figure%
% and write back out as a video file.                                        %
% The calbration corrections use estimates made using the                    %
% Sony37CSHSimpleCalibration.m program.                                      %
%                                                                            %
% Edit all three video files to exactly same frame start using Solveig       %
% Video Splitter which allows perfect cutting before running this code.      %
%                                                                            %
% Calibration made using the underwater tank at SAMS imaging 3 x 44 cm       %
% squares.                                                                   %
% Calibration in E:\UnderwaterCameras\LanderBuildingTestTankCalibrations    %
% each square is in the compiled image 410 pixels square                     %
% NOTE the calibration is slightly different from the vertical stitch        %
% because that program does not rescale the video to .mp4 format.           %
% From the calibration each pixel represents 1.0732 mm                       %
% The FOV of the montaged MP4 image is 1404 x 433 pixels which is            %
% Real world width = ~ 1.5 m swept width Real world height = ~ 0.5 m         %
%                                                                            %
% There is good agreement with the measured distance between the laser       %
% dots which were 130 cm apart on ground at the sled foot level.             %
% On image laser dots are separated by 1199 pixels which = 1,286 mm          %
% The lasers measured on the ground were 1,300 mm apart suggesting           %
% a measurement error of 14 mm over 1.3 m equivalent to 1%.                  %
```

```
% Most razor clams about 19 - 20 cm so measurement error due to image     %
% processing should be 2 mm.                                               %
%%%%%%%%%%%%%%%%%%%%%%%%%%%%%%%%%%%%%%%%%%%%%%%%%%%%%%%%%%%%%%%%%%%%%%%%%%%%%
%%%%%%%%%%%%%%%%%%%%%%%%%%%%%%%%%%%%%%%%%%%%%%%%%%%%%%%%%%%%%%%%%%%%%%%%%%%%%

% Close any old files etc
close all
clc
clear

tic % total elapsed time

% Path to Jaaps lensundistort function
addpath('E:\My Programs\MATLAB\Jaap_LensDistort');
%addpath('I:\My Programs\MATLAB\Jaap_LensDistort');

% Set path where base avi files are located
% Path =
'E:\C0611_FISA_RazorFishSurveys\C0611_Lizanna_Cruise2\RawVideoFiles\';

% Various calibration and alignment test files are in the folder below:-
% Path = 'E:\UnderwaterCameras\LanderBuildingTestTankCalibrations\';
Path =
'E:\UnderwaterCameras\LanderBuildingTestTankCameraHeightCalibration\';
% Path = 'I:\UnderwaterCameras\LanderBuildingTestTankCalibrations\';

%  vid1File = strcat(Path,
'SonyCameraCalibrationRazorSledCruise2SetupCam1.avi');
%  vid2File = strcat(Path,
'SonyCameraCalibrationRazorSledCruise2SetupCam2.avi');
%  vid3File = strcat(Path,
'SonyCameraCalibrationRazorSledCruise2SetupCam3.avi');

% vid1File= strcat(Path, 'Lizanna_Cruise2_Tow9_Camera1.avi');
% vid2File= strcat(Path, 'Lizanna_Cruise2_Tow9_Camera2.avi');
% vid3File= strcat(Path, 'Lizanna_Cruise2_Tow9_Camera3.avi');

vid1File= strcat(Path, 'SonyVN37CSHRHeightCalibration_Part2.avi');
vid2File= strcat(Path, 'SonyVN37CSHRHeightCalibration_Part2.avi');
```

```
vid3File= strcat(Path, 'SonyVN37CSHRHeightCalibration_Part2.avi');

% vid1 = VideoReader(vid1File);
% vid2 = VideoReader(vid2File);
% vid3 = VideoReader(vid3File);

vid1 = VideoReader(vid1File);
vid2 = VideoReader(vid1File);
vid3 = VideoReader(vid1File);

% Set the cruise here to control different camera calibrations
cruise = 0;  % Lander building calibrations in test tank
% cruise = 1; % Lizanna cruise 1
% cruise = 2; % Lizanna cruise 2

% Set skip rate here - processing every frame of video takes a long time
% but skipping leads to video which run very fast and may be hard to
% collect data from

skip = 1;

% Set separate translations on image 1 and 3 to align the composite
% NOTE pos Y values move image downwards neg Y values move image up
% Image 2 is moved to the right over image 1 and image 3 is then moved to
the
% right over the composite of image 1 and 2
% These values may need adjusting for field videos
% to take account of slight movements in the camera brackets as they do not
% affect the image correction to spatial calibration

% Values must be postive >0
if cruise == 0;
    Translate1Y = 20;
    Translate2X = 530;
    Translate2Y = 40;
    Translate3X = 1095;
    Translate3Y = 30;
elseif cruise == 1
    Translate1Y = 20;
```

```
    Translate2X = 535;
    Translate2Y = 20;
    Translate3X = 1095;
    Translate3Y = 1;
elseif cruise == 2
    Translate1Y = 1;
    Translate2X = 530;
    Translate2Y = 10;
    Translate3X = 1085;
    Translate3Y = 1;
end

img1postwarprotate = 0;
img2postwarprotate = 0;
img3postwarprotate = 0;

%%%%% Do not change the parameters below without checking
%%%%% the impact against calibration images
img1prelensdistortresize = [557 792];
img1lensdistort = -0.097;
img1prewarprotate = -1.5;
img1postwarpresize = [620,810];

img2prelensdistortresize = [600 795];
img2lensdistort = -0.096;
img2prewarprotate = -0.5;
img2postwarpresize = [609,805];

img3prelensdistortresize = [600 799];
img3lensdistort = -0.096;
img3prewarprotate = -1;
img3postwarpresize = [617,807];


%***********************************************************************
****
%***********************************************************************
****
```

```
img1 = readFrame(vid1);
img2 = readFrame(vid2);
img3 = readFrame(vid3);

if size(img1,1) ~= 576 && size(img1,2) ~= 944
    promptMessage = sprintf('Warning - Frame size of video 1 does not
appear to be 576x944');
    button = questdlg(promptMessage, 'Continue', 'Continue', 'Cancel',
'Continue');
      if strcmpi(button, 'Cancel')
          return; % Or break or continue
      else
      end
end

if size(img2,1) ~= 576 && size(img2,2) ~= 944
    promptMessage = sprintf('Warning - Frame size of video 2 does not
appear to be 576x944');
    button = questdlg(promptMessage, 'Continue', 'Continue', 'Cancel',
'Continue');
      if strcmpi(button, 'Cancel')
          return; % Or break or continue
      else
      end
end

if size(img3,1) ~= 576 && size(img3,2) ~= 944
    promptMessage = sprintf('Warning - Frame size of video 3 does not
appear to be 576x944');
    button = questdlg(promptMessage, 'Continue', 'Continue', 'Cancel',
'Continue');
      if strcmpi(button, 'Cancel')
          return; % Or break or continue
      else
      end
end

% Check duration here
vid1Info = mmfileinfo(vid1File);
vid2Info = mmfileinfo(vid2File);
```

```
vid3Info = mmfileinfo(vid3File);
vid1Duration = round((vid1Info.Duration/60),2);
vid2Duration = round((vid2Info.Duration/60),2);
vid3Duration = round((vid3Info.Duration/60),2);

promptMessage = sprintf('Duration of video 1 is %2g minutes',
vid1Duration);
button = questdlg(promptMessage, 'Continue', 'Continue', 'Cancel',
'Continue');
      if strcmpi(button, 'Cancel')
          return; % Or break or continue
      else
      end

promptMessage = sprintf('Duration of video 2 is %2g minutes',
vid2Duration);
button = questdlg(promptMessage, 'Continue', 'Continue', 'Cancel',
'Continue');
      if strcmpi(button, 'Cancel')
           return; % Or break or continue
      else
      end

promptMessage = sprintf('Duration of video 3 is %2g minutes',
vid3Duration);
button = questdlg(promptMessage, 'Continue', 'Continue', 'Cancel',
'Continue');
      if strcmpi(button, 'Cancel')
           return; % Or break or continue
      else
      end

clear promptMessage

%%%%%%%%%%%%%%%%%%%%%%%%%%%%%%%%%%%%%%%%%%%%%%%%%%%%%%%%%%%%%%%%%%%%%%%%%%%%
%%%%%%

% new video writer object
```

```
outputVideo = vision.VideoFileWriter('Filename', strcat(Path,
'CompositeVideo.mp4'), 'FileFormat', 'MPEG4');
outputVideo.FrameRate = vid1.FrameRate;

%Note rendering the video out can take some time
% Video will end at point shortest input stream ends

%%%%%%%%%%%%%%%%%%%%%%%%%%%%%%%%%%%%%%
% Define three tforms based on the calibrations made in
% Sony37CSHRSimpleCalibration.m

counter = 0;  % A frame counter - do not change this

img1 = readFrame(vid1);
img2 = readFrame(vid2);
img3 = readFrame(vid3);

%Convert to grayscale - this speeds up the processing
img1=rgb2gray(img1);
img2=rgb2gray(img2);
img3=rgb2gray(img3);

% Prepare 3 tforms - should be possible to reconstruct these from
% data in Sony37CSHRSimpleCalibration but cannto get maketform to work
% properly
img1 = imresize (img1, img1prelensdistortresize);
img1 = lensdistort(img1, img1lensdistort);
img1 = imrotate(img1,img1prewarprotate);
% Negative values in Y move image up
img1X=size(img1,2);
img1Y=size(img1,1);
% This is confusing because images indexed as rows then columns BUT pts
% defined as X then Y i.e. Columns then Rows
% Pairs as Top-left; Mid-left; bottom-left;  top-mid; centre; bottom-mid;
% top-right; mid-right; bottom right
movingPts1 = [1 1; 1 img1Y/2; 1 img1Y; img1X/2 1; img1X/2 img1Y/2; img1X/2
img1Y; img1X 1; img1X img1Y/2; img1X img1Y];
% Now define where we want them to end up
targetPts1 = [-40 50; 17 img1Y/2+10; -5 img1Y+60; img1X/2+5 1; img1X/2
img1Y/2; img1X/2 img1Y-30; img1X+10 20; img1X img1Y/2; img1X img1Y+70];
```

```
% This should shift the top left corner down a bit
tform1 = fitgeotrans(movingPts1, targetPts1, 'projective');
img1 = imwarp(img1, tform1);
img1 = imresize(img1,img1postwarpresize);
img1 = imrotate(img1,img1postwarprotate);
%imtool(img1)

img2 = imresize (img2, img2prelensdistortresize);
img2 = lensdistort(img2, img2lensdistort);
img2 = imrotate(img2,img2prewarprotate);
img2X = size(img2,2);
img2Y = size(img2,1);
% Negative values in Y move image up
movingPts2 = [1 1; 1 img2Y/2; 1 img2Y; img2X/2 1; img2X/2 img2Y/2; img2X/2
img2Y; img2X 1; img2X img2Y/2; img2X img2Y];
% Now define where we want them to end up;
targetPts2 = [1 -10; 1 img2Y/2; 1 img2Y+30; img2X/2 25; img2X/2-25
img2Y/2+15; img2X/2 img2Y; img2X+50 1; img2X-50 img2Y/2; img2X+60 img2Y];
% This should shift the top left corner down a bit
tform2 = fitgeotrans(movingPts2, targetPts2, 'projective');
img2 = imwarp(img2, tform2);
img2 = imresize(img2,img2postwarpresize);
img2 = imrotate(img2,img2postwarprotate);
%imtool(img2)

img3 = imresize (img3, img3prelensdistortresize);
img3 = lensdistort(img3, img3lensdistort);
img3 = imrotate(img3,img3prewarprotate);
% Negative values in Y move image up
img3X = size(img3,2);
img3Y = size(img3,1);
movingPts3 = [1 1; 1 img3Y/2; 1 img3Y; img3X/2 1; img3X/2 img3Y/2; img3X/2
img3Y; img3X 1; img3X img3Y/2; img3X img3Y];
% Now define where we want them to end up
targetPts3 = [1 1; 1 img3Y/2; 1 img3Y; img3X/2 1; img3X/2 img3Y/2; img3X/2
img3Y; img3X -15; img3X img3Y/2; img3X+10 img3Y];
% This should shift the top left corner down a bit
tform3=fitgeotrans(movingPts3, targetPts3, 'projective');
img3=imwarp(img3, tform3);
img3 = imresize(img3,img3postwarpresize);
```

```
img3 = imrotate(img3,img3postwarprotate);
%imtool(img3)
% These vertices help with placing the compiled image for the lower panel
into the
% final composition frame
% The -1 is needed because the origin on imgh is at a zero but indexing in
% img starts at 1
imgh1TopY = 600+Translate1Y;
imgh1BottomY = imgh1TopY+size(img1,1)-1;
imgh1LeftX = 250;
imgh1RightX = imgh1LeftX+size(img1,2)-1;

img1TopY = 1;
img1BottomY = size(img1,1);
img1LeftX = 1;
img1RightX = size(img1,2);

imgh2TopY = 600+Translate2Y;
imgh2BottomY = imgh2TopY+size(img2,1)-1;
imgh2LeftX = imgh1LeftX+Translate2X+50;
imgh2RightX = imgh2LeftX+size(img2,2)-50;

img2TopY = 1;
img2BottomY = size(img2,1);
img2LeftX = 50;
img2RightX = size(img2,2);

imgh3TopY = 600+Translate3Y;
imgh3BottomY = imgh3TopY+size(img3,1)-1;
imgh3LeftX = imgh1LeftX+Translate3X+50;
imgh3RightX = imgh3LeftX+size(img3,2)-50;

img3TopY = 1;
img3BottomY = size(img3,1);
img3LeftX = 50;
img3RightX = size(img3,2);

clear targetPts1 targetPts2 targetPts3 movingPts1 movingPts2 movingPts3;
clear vid1Duration vid2Duration vid3Duration
```

```
vid1 = VideoReader(vid1File);
vid2 = VideoReader(vid2File);
vid3 = VideoReader(vid3File);

%Preallocate imgh to save time reading and writing - this is the max size
%for an MP4 video
imgh = zeros(1088, 1920, 'uint8');

% new video writer object
outputVideo = vision.VideoFileWriter('Filename', strcat(Path,
'CompositeVideo.mp4'), 'FileFormat', 'MPEG4');
outputVideo.FrameRate = vid1.FrameRate;

%while hasFrame(vid1) && hasFrame(vid2)&& hasFrame(vid3)
    while hasFrame(vid1) && hasFrame(vid3)


        counter=counter+1;      %Set counter for numbering output frames

        img1 = readFrame(vid1);
        img2 = readFrame(vid2);
        img3 = readFrame(vid3);

        %Convert to grayscale - this speeds up the processing
        img1=rgb2gray(img1);
        img2=rgb2gray(img2);
        img3=rgb2gray(img3);

        % Some checks only on first frameset
        if counter == 1;

        if (vid1.framerate == vid2.framerate)&&(vid1.framerate ==
vid3.framerate)&&(vid2.framerate == vid3.framerate)
        %Images are same size
        else

        %Images are not same framerate - I have no idea why the DVR would
do this but it
```

```
        %seemed to occur in some recordings - perhaps something set
inconsistently
        %in camera settings on DVR
        promptMessage = 'Images do not have a consistent framerate, do you
want to continue or Cancel to abort processing? Feed 1';
        button = questdlg(promptMessage, 'Continue', 'Continue', 'Cancel',
'Continue');
            if strcmpi(button, 'Cancel')
                return; % Or break or continue
            else
                %Easiest option is to re-export original files with correct
                %framerate using ImageShare Video Converter. No easy way to
redo
                %framerates in Matlab
            end
        end

        %Check size of all images is same
        Heights(1)=size(img1,1);
        Widths(1)=size(img1,2);
        Heights(2)=size(img2,1);
        Widths(2)=size(img2,2);
        Heights(3)=size(img3,1);
        Widths(3)=size(img3,2);

        if (Heights(1) == Heights(2))&&(Heights(1) ==
Heights(3))&&(Heights(2) == Heights(3))&& ...
             (Widths(1) == Widths(2))&&(Widths(1) == Widths(3))&&(Widths(2)
== Widths(3));
             %Images are same size
        else

         %Images are not same size - I have no idea why the DVR would do
this but it
         %seemed to occur in some recordings - perhaps something set
inconsistently
         %in camera settings - ideally all cameras same res output because
rescaling
         %leads to some additional image distortion
```

```
        promptMessage = 'Images not consistent size, do you want to
rescale,\nor Cancel to abort processing?';
        button = questdlg(promptMessage, 'Continue', 'Continue', 'Cancel',
'Continue');
            if strcmpi(button, 'Cancel')
                return; % Or break or continue
            else

                %Find max size
                MaxHeight=max(Heights);
                MaxWidth=max(Widths);

                img1=imresize(img1, [MaxHeight MaxWidth]);
                img2=imresize(img2, [MaxHeight MaxWidth]);
                img3=imresize(img3, [MaxHeight MaxWidth]);

            end

        end

    end

    % If skipframes <>1 then this step determines which frames to process
    if rem(counter, skip) == 0

        img1 = imresize (img1, img1prelensdistortresize);
        img1 = lensdistort(img1, img1lensdistort);
        img1 = imrotate(img1,img1prewarprotate);
        img1 = imwarp(img1, tform1);
        img1 = imresize(img1,img1postwarpresize);
        img1 = imrotate(img1,img1postwarprotate);

        img2 = imresize (img2, img2prelensdistortresize);
        img2 = lensdistort(img2, img2lensdistort);
        img2 = imrotate(img2,img2prewarprotate);
        img2 = imwarp(img2, tform2);
        img2 = imresize(img2,img2postwarpresize);
        img2 = imrotate(img2,img2postwarprotate);
```

```
        img3 = imresize (img3, img3prelensdistortresize);
        img3 = lensdistort(img3, img3lensdistort);
        img3 = imrotate(img3,img3prewarprotate);
        img3 = imwarp(img3, tform3);
        img3 = imresize(img3,img3postwarpresize);
        img3 = imrotate(img3,img3postwarprotate);

        % Place img1 in the top left corner - NOTE array is row (Y) then
        % column (X) whereas an image is indexed as X (column) then Y
(rows)
        imgh(1:size(img1,1),1:size(img1,2)) = img1;
        %Place img2 in top centre
        XShift = size(img1,2) + 10;
        imgh(Translate2Y:(Translate2Y+size(img2,1)-
1),XShift:(XShift+size(img2,2)-1)) = img2;
        % Place img3 in the top right corner - NOTE array is row (Y) then
        % column (X) whereas an image is indexed as X (column) then Y
(rows)
        XShift = XShift + size(img2,2) + 10;
        imgh(Translate3Y:(Translate3Y+size(img3,1)-
1),XShift:(XShift+size(img3,2)-1)) = img3;
        % Create a second montaged image to run below the separate images
        % Use the vertices calculated before the loop to reduce processing
        % time
        imgh(imgh1TopY:imgh1BottomY,imgh1LeftX:imgh1RightX) =
img1(img1TopY:img1BottomY,img1LeftX:img1RightX);
        imgh(imgh2TopY:imgh2BottomY,imgh2LeftX:imgh2RightX) =
img2(img2TopY:img2BottomY,img2LeftX:img2RightX);
        imgh(imgh3TopY:imgh3BottomY,imgh3LeftX:imgh3RightX) =
img3(img3TopY:img3BottomY,img3LeftX:img3RightX);

        % Rescale image to Windows MP4 format max which is max 1088 x 1920
        % This does mean we lose a few pixels in the width dimension
        % using NaN preserves the aspect ratio
        imgh=imresize(imgh, [NaN 1920]);

        %Blank out borders to give width 1.5 m width on image
        % As Y origin to Y end , X origin to X end
        if cruise == 0;  % Lander building calibrations
            % Vertical left
```

```
    imgh(1:size(imgh,1), 1:10)=0;
    imgh(470:size(imgh,1), 1:200)=0;
    % Horizontal top
    imgh(1:20, 1:size(imgh,2))=0;
    % Horizontal mid
    imgh(470:510, 1:size(imgh,2))=0;
    % Horizontal bottom
    imgh(960:size(imgh,1), 1:size(imgh,2))=0;
    % Vertical right
    imgh(1:size(imgh,1), (size(imgh,2)-10):size(imgh,2))=0;
    imgh(470:size(imgh,1), (size(imgh,2)-250):size(imgh,2))=0;
    % Vertical mid X img1 img2 Top row
    imgh(1:470,600:650)=0;
    % Vertical mid X img2 img3 Top row
    imgh(1:470,1260:1310)=0;

elseif cruise == 1
    % Vertical left
    imgh(1:size(imgh,1), 1:40)=0;
    imgh(470:size(imgh,1), 1:230)=0;
    % Horizontal top
    imgh(1:20, 1:size(imgh,2))=0;
    % Horizontal mid
    imgh(450:510, 1:size(imgh,2))=0;
    % Horizontal bottom
    imgh(910:size(imgh,1), 1:size(imgh,2))=0;
    % Vertical right
    imgh(1:size(imgh,1), (size(imgh,2)-70):size(imgh,2))=0;
    imgh(470:size(imgh,1), (size(imgh,2)-250):size(imgh,2))=0;
    % Vertical mid img1 img2 Top row
    imgh(1:470,600:650)=0;
    % Vertical mid X img2 img3 Top row
    imgh(1:470,1260:1310)=0;
elseif cruise == 2
     % Vertical left
    imgh(1:size(imgh,1), 1:40)=0;
    imgh(470:size(imgh,1), 1:230)=0;
    % Horizontal top
    imgh(1:80, 1:size(imgh,2))=0;
    % Horizontal mid
```

```
            imgh(450:550, 1:size(imgh,2))=0;
            % Horizontal bottom
            imgh(940:size(imgh,1), 1:size(imgh,2))=0;
            % Vertical right
            imgh(1:size(imgh,1), (size(imgh,2)-70):size(imgh,2))=0;
            imgh(470:size(imgh,1), (size(imgh,2)-290):size(imgh,2))=0;
            % Vertical mid img1 img2 Top row
            imgh(1:470,600:650)=0;
            % Vertical mid X img2 img3 Top row
            imgh(1:470,1260:1310)=0;
        end

        %Ask user if OK to proceed with video merging
        if counter ==1
            imtool(imgh);

            promptMessage = sprintf('Do you want to Continue
processing,\nor Cancel to abort processing?');
            button = questdlg(promptMessage, 'Continue', 'Continue',
'Cancel', 'Continue');
            if strcmpi(button, 'Cancel')
                return; % Or break or continue
            end
        end

        toc      % Without warping about 1.7 s per frame, with warping 2.3
seconds
                 % so to render 1 h of video at full fps will take  42
                 % HOURS! OK I suppose as long as program doesn't crash
        counter  % Show frame being processed in cmd window

        % record new video
        step(outputVideo, imgh);
    end

end

release(outputVideo);
```

Appendix 2

Matlab code to generate a vertically stitched image from a single camera feed and to estimate the distance over the ground that the camera has been towed over.

```
%%%%%%%%%%%%%%%%%%%%%%%%%%%%%%%%%%%%%%%%%%%%%%%%%%%%%%%%%%%%%%%%%%%%%%%%%%%%
%   PROGRAM BY: Clive Fox, Nov 2016                                        %
%   FILE NAME: VerticalStitching
%
%   DESCRIPTION: Takes output from single towed Sony37CSHS camera, convert%
%   convert to real world calibrated image, combine vertically to allow   %
%   distance travelled to be estimated against video timestamps.           %
%                                                                          %
%   The calibration corrections use estimates made using the
%
%   Sony37CSHSimpleCalibration.m program.                                  %
%                                                                          %
%   If there are gaps in the video the program will halt at that point.   %
%   From the calibration squares recorded in the lander test tank          %
%   each pixel thus represents 1.0864 mm in this program.                  %
%   Each stitched section indicated by short gray bar at side of image    %
%   Each 0.5 m marked with short white bar, each 1 m with longer white bar%
%%%%%%%%%%%%%%%%%%%%%%%%%%%%%%%%%%%%%%%%%%%%%%%%%%%%%%%%%%%%%%%%%%%%%%%%%%%%
%%%%%%%%%%%%%%%%%%%%%%%%%%%%%%%%%%%%%%%%%%%%%%%%%%%%%%%%%%%%%%%%%%%%%%%%%%%%


% Close any old files etc
close all
clc
clear

% Path to Jaaps lensundistort function
addpath('E:\My Programs\MATLAB\Jaap_LensDistort');
%addpath('I:\My Programs\MATLAB\Jaap_LensDistort');

%Set path where base .avi files are located
Path =
'E:\C0611_FISA_RazorFishSurveys\C0611_Lizanna_Cruise2\RawVideoFiles\';
% Path = 'E:\My
Programs\MATLAB\RazorClamsVideoProcessing\VerticalMontage\';
%Path = 'I:\My Programs\MATLAB\RazorClamsVideoProcessing\VerticalMontage\';
```

```
inputVideoFile = strcat(Path, 'Lizanna_Cruise2_Tow4_Camera2.avi');

% Below is just a still calibration image to check distortion corrections
% The square is 44 cm internal width and height
% inputVideoFile = strcat(Path, 'DemoSonyCameraCalibration.avi');

%Set skip rate here - montaging every frame of video takes too long, adjust
%the skip value to balance combineImg quality and speed

Skip = 1;  % Saves every nth frame i.e. if video is 21 frames per sec then
            % equates to saving a composite image every 1 s if framerate is
            % 21 per second - processing
            % every frame gives best result but will be very slow
            % Skip must be integer >0

% Adjust if camera is rotated but large corrections may
% mess up the auto combineImg
imagepostwarprotate = 1;


%%%%% Do not change the parameters below without checking
%%%%% the impact against calibration images
imageprelensdistortresize = [600 792];
imagelensdistort = -0.097;
imageprewarprotate = -1.5;
imagepostwarpresize = [615,810];
% Pixel to real world conversion - pixels to mm
% NOTE this is slightly different to the calibration used
% in the horizontal montage program because that program
% rescales the final image to .mp4 format
% In this program 44 cm calibration squares = 405 pixels
pixelCal = 1.08642;

% Preallocate memory for results - array should be large enough for a 200m
% tow, longer tows may give error and this number need increasing
n=200000;

% Array to hold montaged image for checking stitching quality - size set to
% about 200 m tow max.
montageImg=zeros(n,810, 'uint8');
results = struct('DistPix',zeros(1,n),'Distm',zeros(1,n), ...
    'Frame',zeros(1,n),'VideoTime',zeros(1,n));

%*************************************************************************

%*************************************************************************


frameCounter = 2;     % A frame counter - do not change this
resultCounter = 1; %A counter for results - if skip used then number of
results<frames
distCounter=0.5; %A counter to track 0.5 an 1 m marks


videoObject = VideoReader(inputVideoFile);
% Check duration here, total frames and framerate
videoObjectInfo = mmfileinfo(inputVideoFile);
videoObjectDuration = round((videoObjectInfo.Duration/60),2);
numberOfFrames=videoObject.numberOfFrames;
```

```
frameRate=videoObject.frameRate;

% Note have to recreate videoReader after using NumberOfFrames
videoObject = VideoReader(inputVideoFile);
image = readFrame(videoObject);

if size(image,1) ~= 576 && size(image,2) ~= 944
    promptMessage = sprintf ...
        ('Warning - Frame size of video 1 does not appear to be 576x944');
    button = questdlg ...
        (promptMessage, 'Continue', 'Continue', 'Cancel', 'Continue');
      if strcmpi(button, 'Cancel')
          return; % Or break or continue
      else
      end
end

promptMessage = sprintf ...
    ('Duration of video 1 is %2g minutes', videoObjectDuration);
button = questdlg ...
(promptMessage, 'Continue', 'Continue', 'Cancel', 'Continue');
if strcmpi(button, 'Cancel')
      return; % Or break or continue
else
end

fixedImg = readFrame(videoObject);
%Convert to grayscale - this speeds up the processing
fixedImg=rgb2gray(fixedImg);

% Remove and store video timestamps before image distortion is corrected
% imcrop is [xmin ymin width height]  - origin is at top left
timeStamp = imcrop(fixedImg,[460,10,180,30]);
% Pick up start time on video - cannot machine read this
imshow(timeStamp)

% Uncomment testline below before use
ok=0;
while ok == 0
    startTime=inputdlg ...
    ('Please enter video start date and 24 h time from the timestamp shown
as dd/MM/yyyy HH:mm:ss', ...
    'Start time',1);
    if isempty(startTime)
        % Leave ok as zero
    else
        try
            datetime(startTime,'InputFormat','dd/MM/yyyy HH:mm:ss');
            ok=1;
        catch
            % Invalid datetime format - leave ok as zero
        end
    end
end

startTime=datetime(startTime, 'InputFormat','dd/MM/yyyy HH:mm:ss');

% Define a tform based on the calibrations made in
% Sony37CSHRSimpleCalibration.m
```

```
fixedImg = imresize (fixedImg, imageprelensdistortresize);
fixedImg = lensdistort(fixedImg, imagelensdistort);
fixedImg = imrotate(fixedImg,imageprewarprotate);
% Negative values in Y move image up
fixedImgX=size(fixedImg,2);
fixedImgY=size(fixedImg,1);
% This is confusing because images indexed as rows then columns BUT pts
% defined as X then Y i.e. Columns then Rows
% Pairs as Top-left; Mid-left; bottom-left;  top-mid; centre; bottom-mid;
% top-right; mid-right; bottom right
movingPts1 = [1 1; 1 fixedImgY/2; 1 fixedImgY; fixedImgX/2 1; ...
    fixedImgX/2 fixedImgY/2; ...
    fixedImgX/2 fixedImgY; fixedImgX 1; ...
    fixedImgX fixedImgY/2; fixedImgX fixedImgY];
% Now define where we want them to end up
targetPts1 = [-40 50; 17 fixedImgY/2+10; -5 fixedImgY+60; ...
    fixedImgX/2+5 1; fixedImgX/2 fixedImgY/2; ...
    fixedImgX/2 fixedImgY-30; fixedImgX+10 20; ...
    fixedImgX fixedImgY/2; fixedImgX fixedImgY+70];

% This should shift the top left corner down a bit
tform1 = fitgeotrans(movingPts1, targetPts1, 'projective');
fixedImg = imwarp(fixedImg, tform1);
fixedImg = imresize(fixedImg,imagepostwarpresize);
fixedImg = imrotate(fixedImg,imagepostwarprotate);
% Then need to rescale image so that the 44 cm calibration squares
% are 405 pixels - this then matches the scaling in the Horizontal
% combineImg program
fixedImg=imresize(fixedImg, [NaN 640]);
% imtool(fixedImg);
% Should produce an image where 44 cm calibration squares produce
% square 520 pixels - this can be checked using the
% file DemoSonyCamera.avi
% NOTE this calibration is different to that in horizontal montage
% because that program rescales final image to .mp4 format

% Trim off the timestamp and cam label which causes problems with the auto-
combineImg
% [xmin ymin width height]  - origin is at top left
fixedImg = imcrop(fixedImg,[50, 60,
(size(fixedImg,2)),(size(fixedImg,1))]);
```

```
clear('fixedImgX','fixedImgY');

% Put image and timestamp into montage array
montageImg(1:(size(fixedImg,1)), ...
            (size(montageImg,2)-size(fixedImg,2)+1):size(montageImg,2))=
...
            fixedImg;
montageImg(1:size(timeStamp,1), ...
        1:(size(timeStamp,2))) = timeStamp;

% This counter for the row number of the top of the image, we add vertShift
% to this later on
rowsShifted=0;

% try
while hasFrame(videoObject)


    if rem(frameCounter,Skip) == 0 % We are at frame set by skip rate so
process this frame

        % Read next frame in video
        movingImg = readFrame(videoObject);
        % Convert video frame to grayscale - feature detection does not
work on RGB
        movingImg=rgb2gray(movingImg);

        % Remove and store video timestamps before image distortion is
corrected
        % imcrop is [xmin ymin width height]  - origin is at top left
        timeStamp = imcrop(movingImg,[460,10,180,30]);

        % Correct image for camera distortion
        movingImg = imresize (movingImg, imageprelensdistortresize);
        movingImg = lensdistort(movingImg, imagelensdistort);
        movingImg = imrotate(movingImg,imageprewarprotate);
        movingImg = imwarp(movingImg, tform1);
        movingImg = imresize(movingImg,imagepostwarpresize);
        movingImg = imrotate(movingImg,imagepostwarprotate);
```

```
        movingImg = imresize(movingImg, [NaN 640]);
        % imcrop[xmin ymin width height]
        movingImg = imcrop(movingImg,[50, 60,
(size(movingImg,2)),(size(movingImg,1))]);

        % movingImg and fixedImg should now be same size and distortion
        % corrected

        ptsfixedImg = detectSURFFeatures(fixedImg);
        ptsmovingImg = detectSURFFeatures(movingImg);

        % Check we have enough points
        if length(ptsmovingImg)<5
            % Not enough points so skip frame
            % hopefully next frame will have enough information
            continue
        end

        % Extract the feature descriptors
        [featuresfixedImg, ptsfixedImg] = extractFeatures(fixedImg,
ptsfixedImg);
        [featuresmovingImg, ptsmovingImg] = extractFeatures(movingImg,
ptsmovingImg);

        % Match features
        indexPairs = matchFeatures(featuresfixedImg, featuresmovingImg);

        matchedfixedImg  = ptsfixedImg(indexPairs(:,1));
        matchedmovingImg = ptsmovingImg(indexPairs(:,2));

        % Statistically remove outliers using MSAC algorithm and the most
basic
        % transform
        [tform, inliermovingImg, inlierfixedImg] = ...
            estimateGeometricTransform(matchedmovingImg, ...
            matchedfixedImg,'similarity');

        % Un-comment lines below to check transformation
        % figure;
```

```
        % showMatchedFeatures(fixedImg,movingImg, inlierfixedImg,
inliermovingImg);
        % title('Matching points (inliers only)');
        % legend('ptsfixedImg','ptsmovingImg');

        % Now the tform object contains the transform but we know that
images
        % should only shift downwards as the camera rig is towed along
        % So start of tow will be at top of final composite image
        % We need to retain top part of the fixedImg image, and merge the
movingImg image
        % then save that as the combineImg which we will build up
        % If this is not working check that on the video the objects are
        % moving from bottom to top.

        % From the affine transformation the y displacement is cell [3,2]
        % In my tests there was a slight x displacement and a minor scaling
        % indicated by non - 1 values on the matrix diagonal
        % http://uk.mathworks.com/discovery/affine-transformation.html

        % Extend the fixedImg at bottom by vertical shift
        % based on tform.T(3,2)
        vertShift = double(round(tform.T(3,2),0));

        % Build up the montage array - dist shifted in metres
        rowsShifted=rowsShifted+vertShift;

        if rowsShifted==0
            montageImg(1: ...
            (rowsShifted+size(movingImg,1)), ...
            (size(montageImg,2)-size(movingImg,2)+1): ...
            size(montageImg,2))= movingImg;
        else
        montageImg(rowsShifted: ...
            (rowsShifted+size(movingImg,1)-1), ...
            (size(montageImg,2)-size(movingImg,2)+1): ...
            size(montageImg,2))= movingImg;
        end

        % Put stitch and distance flags into montage
        midImg=round((size(movingImg,1)/2),0);
        pixShifted=rowsShifted+midImg;
        distShifted=round((pixShifted*pixelCal/1000),3);

        %Detect each time distShifted goes over 0.5 or 1 m
        if distShifted > distCounter
            if rem(distCounter,1)==0
                % Put long white mark at each meter - measured from
                % centre of image
                montageImg(rowsShifted:(rowsShifted+1), ...
                    (size(montageImg,2)-size(movingImg,2)-50): ...
                    (size(montageImg,2)-size(movingImg,2)-1))=256;
                distCounter=distCounter+0.5;
            elseif rem(distCounter,0.5)==0
                % Put short white mark at each half meter
                montageImg(rowsShifted:(rowsShifted+1), ...
                    (size(montageImg,2)-size(movingImg,2)-25): ...
                    (size(montageImg,2)-size(movingImg,2)-1))=256;
                distCounter=distCounter+0.5;
```

```
    end
else
    if rowsShifted==0
        % do not mark
    else
    % Put short grey mark at each stitch
    montageImg(rowsShifted:(rowsShifted+1), ...
        (size(montageImg,2)-size(movingImg,2)-25): ...
        (size(montageImg,2)-size(movingImg,2)-1))=120;
    end
end

% Add timestamp every 30 seconds of elapsed video
%Must round to hundredths of seconds otherwise elapsedTime
% never exactly equals unity
elapsedTime = round(frameCounter/(frameRate),2);
if rem(elapsedTime,30)==0
montageImg(rowsShifted:(rowsShifted+size(timeStamp,1)-1), ...
        1:(size(timeStamp,2))) = timeStamp;
end
```

```
        % Display developing montage
        if rowsShifted<576
            imshow(montageImg(1:size(movingImg,1),1:size(montageImg,2)));
        else
            imshow(montageImg((rowsShifted-200): ...
                (rowsShifted+375), ...
                1:size(montageImg,2)));
        end

        % Record the distance, frame etc, measured from centre of
        % the moving image
        results.DistPix(resultCounter)=pixShifted;
        results.Distm(resultCounter)=distShifted;
        results.Frame(resultCounter)=frameCounter;
        % elapsed time previously calculated in seconds - convert to
        % fraction of a day
            elapsedTime=elapsedTime/86400;
        obsTime=datenum(startTime)+elapsedTime;
        results.VideoTime(resultCounter)=obsTime;
        resultCounter=resultCounter+1;

        % Save movingImage as next fixedImage
        fixedImg=movingImg;

    else

       Rubbish = readFrame(videoObject);

    end
    %Increment the frame counter
    frameCounter=frameCounter+1;

    percentComplete=frameCounter/numberOfFrames*100;

    % Track progress
    frameCounter
    percentComplete

end
```

```
saveFile= strcat(Path, 'VerticalMonatageResults.txt');

fid=fopen(saveFile, 'wt') ;
% \t=tab   \n new line %s string
fprintf(fid, '%s \t%s\n\n', 'Distance estimate from video file ', ...
    inputVideoFile);
fprintf(fid, '%s \t\t%s \t%s
\t%s\n','Frame','Dist_pix','Dist_m','VideoTime');

for counter=1:resultCounter
    fprintf(fid, '%i \t\t%g \t%g \t%s \n', ...
    results.Frame(counter), ...
    results.DistPix(counter),...
    results.Distm(counter),  ...
    datestr(results.VideoTime(counter)));
end
fclose(fid);

% Clean off unused part of array and save montage as a png
montageImg=montageImg(1:(rowsShifted+size(movingImg,1)-
1),1:size(montageImg,2));
imwrite(montageImg, strcat(Path,'Montage.png'));
```

Appendix 3

Matlab code for the GUI program allowing measurement of objects on video. The GUI requires both a .fig file and a .m file to be installed so the code is not listed here. The two parts of the program are available to download from http://uk.mathworks.com/matlabcentral/fileexchange/61356-measure-objects-on-video.

A run-time version can be supplied by C Fox on request which allows users to install and run the program without having Matlab installed on their PC.